Study on Effective Utilization of Goethite-based Nanoporous Ore

ナノ多孔質ゲーサイト基鉱石の有効利用に関する研究

by Keisuke ABE

Chapter 1

General Introduction

1-1. Background; Ironmaking problems about Resource, Environment, and Energy

1-1-1. Resource problems in the ironmaking industry: high-grade ore and coal

Iron is fourth the most abundant element in the earth's crust after O, Si, and Al ones. Because of the abundance in resource, good mechanical property, and easy reduction process, iron is the most produced metal in the world. Recent worldwide economic growth causes the demand expansion of iron. The amount of iron production has been increasing year by year in the world, resulting in resource problem in the iron and steel industry.

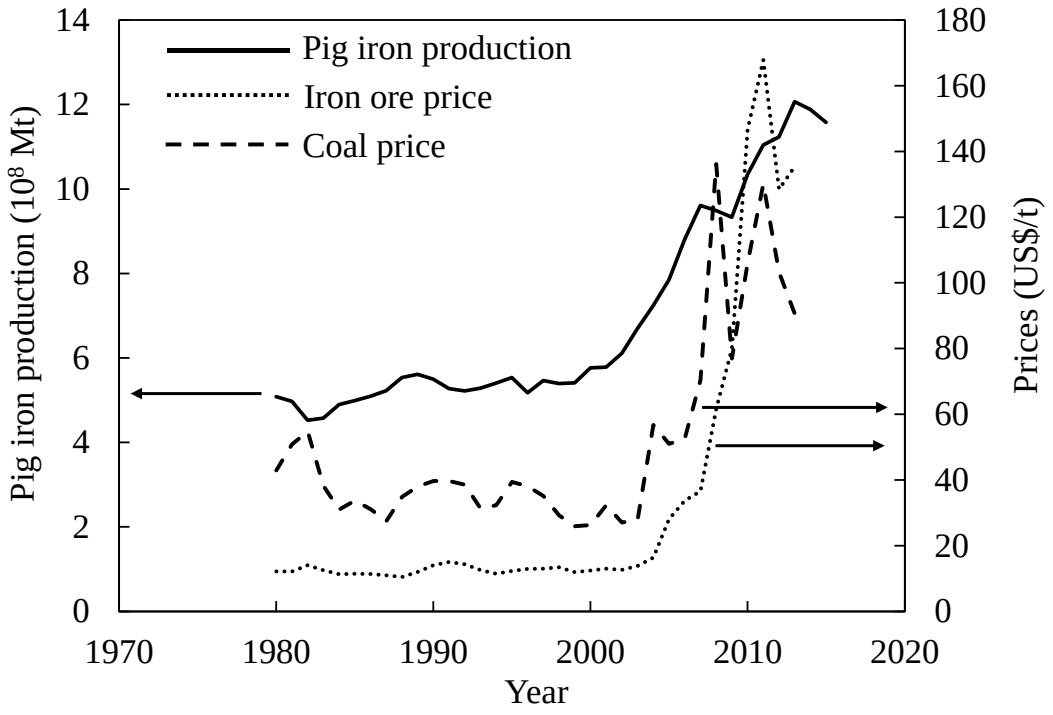

Figure 1-1. The amount of pig iron produced in the world and the prices of the high-grade iron ore and coal [1-4].

In the actual blast furnace ironmaking process, high-grade iron ore (sinter ore), coke (produced from strongly caking coal), and limestone are utilized to produce pig iron. As shown in Figure 1-1, the amount of pig iron production has been rapidly increasing worldwide. This causes degradation and high-price of the high-grade iron ore. Yearly transition of the prices of iron ore and coal are also shown in Figure 1-1. The iron ore in this figure was that imported by China and contained 62mass% of Fe. The coal, which was produced in Australia, contained 14mass% of ash and 1mass% of sulfur. The price

of the high grade iron ore has been rising from 14 USD/t in 1990 to 130 USD/t in 2013. New iron ore resources which are abundant and cheap are highly needed to decrease the cost of raw materials. One of the alternate iron ore is goethite (FeOOH) ore in Southeastern Asia and Oceania contains less than 60wt% of iron. The FeOOH contains combined water, which causes pulverization due to heating, makes it difficult to put the goethite ore directly into the blast furnace. That is why, the goethite ore is sent to a sintering process to remove the combined water to obtain high-strength sintered ore. Coke, which works as a heat source, reducing agent, and maintaining the gas flow in the blast furnace, is produced from coal by heating at 1200℃ for 20 h without oxygen.

1-1-2. Environmental problem in the ironmaking industry: large amount of CO_2 emission

The iron and steel industry has an environmental problem related to CO_2 emission. CO_2 is mainly emitted in the iron and steel industry due to combustion of fossil fuels for heat sources and production of electrical energy, reduction process of iron ores to pig iron, and final steel production. Figure 1-2 (A) shows the CO_2 emission in the worldwide iron and steel industry and the CO_2 emission ratio of the iron and steel industry to the world CO_2 emission related to fuel combustion [5-7]. CO_2 emission in the world iron and steel industry has been increasing year by year. The contribution of the CO_2 emission in the iron and steel industry to the world CO_2 emission has been also increasing; around

9% of the total CO_2 emission is contributed by this industry. In the iron and steel industry, CO_2 emissions in the processes related to blast furnace account for around 50% of the total emissions.

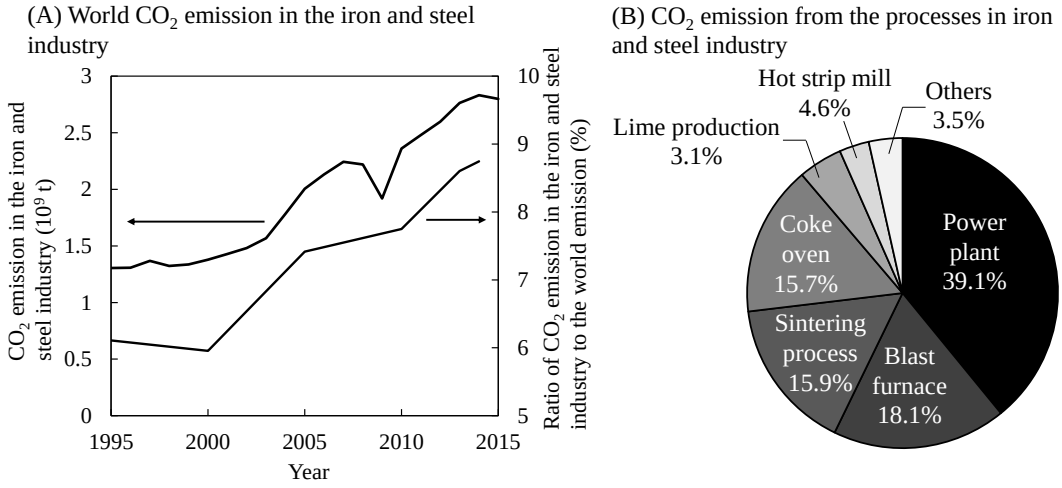

Figure 1-2 CO_2 emissions in the iron and steel industry [5-7]. (A): the amount and the ratio of CO_2 emission in the iron and steel industry and (B): CO_2 amount from each process in the iron and steel industry.

1-1-3. Energetic problems in the ironmaking industry: emission of high-temperature waste heat

The iron and steel industry is one of the most energy-consuming industries. The industry used 2.3×10^{19} J in 2005 which was the second largest amount of energy

usage among all industries [8]. This means that the iron and steel industry has potential to play a significant role for energy saving especially in blast furnace and coke oven processes. Because of the large amount of energy usage, the iron and steel industry emits a lot of waste heat without effective recovery. Figure 1-3 shows the examples of the amount of waste heat in the iron and steel industry [9]. The amount of unutilized waste heat based on enthalpy is higher at lower temperatures. However, the quality of the heat energy, as it is called "exergy", is much larger at higher temperatures. The heat exergy is expressed as a function of temperature T:

$$\text{Heat exergy} = 1 - \frac{T_0}{T} \quad (1\text{-}1)$$

where T_0 is environmental temperature (298 K). It is obvious from the equation (1-1) that the heat exergy becomes larger at higher temperatures. That is why the amount of waste heat based on exergy is much larger at high temperature regardless of larger enthalpy at lower temperatures. This means high-temperature waste heat has a potential to be more effectively utilized.

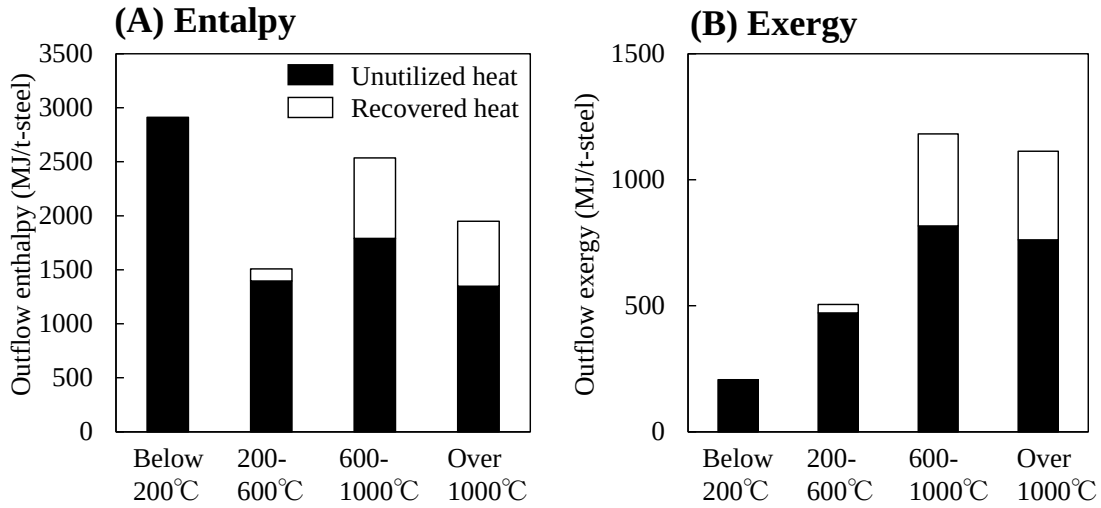

Figure 1-3 The amount of waste heat in the iron and steel industry [9].

1-2. Goethite ore

The goethite-based (FeOOH) iron ore is abundant in South-East Asia and Oceania but ineffectively utilized because the ore has a lot of (approximately 10mass%) combined water (CW) inside it. In the actual ironmaking process, the goethite ore is sintered with coke powder and lime at over 1400 ℃ for high strength. It is already known that nanoporous Fe_2O_3 can be obtained by the dehydration process with mild calcination at low temperature [10-16].

$$2FeOOH\ (s) \rightarrow Fe_2O_3\ (s) + H_2O\ (g) \qquad (1\text{-}2)$$

The porous structure of the calcined goethite has been investigated by a lot of researchers; the pore structure changes by the calcination temperature [10-16]. At lower temperature (200-300℃) of calcination layered slit-type micropores and mesopores are generated [10, 13-16]. Dehydration reaction occurs at around 250℃ and combined water comes out from goethite [15], resulting in micropores (around 1 nm) in the dehydrated goethite. The mesopores are said to be generated by the removal of water molecules between initial crystalline of the goethite [15]. When the calcination temperature becomes higher (500-600℃) the pores get larger and become spherical shape [10, 13]. Calcination temperature of over 800℃ destroyes the pore structure of

the goethite [16].

The goethite has an interesting property to become nanoporous material as mentioned above, however, the goethite ore in the actual process is treated at high temperature (over 1400℃) only to satisfy the demand of the blast furnace. At the high temperature, the nanopores in the goethite ore are completely destroyed.

1-3. Limonite ore (Ni-containing goethite-based ore) utilization as a catalyst

1-3-1. Ni-containing goethite ore (limonite ore) in the laterite soil

Ni is widely utilized in a lot of products such as catalysts and stainless steel. The smelting of Ni is taken place from two types of Ni ores; oxide ore and sulfide ore. Reserve estimation says that Ni oxide ore accounts for around 72% of the total ores. From the view point of Ni resource, oxide ore is much more abundant in the earth, however, sulfide ore is mainly utilized for Ni production; 58% of the Ni in the world is made from the sulfide ore [17]. That is because it is possible only for sulfide ores to condensate Ni component via flotation separation [18]. The Ni oxide ores are not used often for the production of Ni. That is why, they have potential to be used in another method. Ni oxide ores are mainly existed in laterite soil in the south-eastern Asia and Oceania areas. Figure 1-4 Shows the schematic image of the laterite soil. In the laterite soil, there are mainly three types of zone; the limonite zone, the transition zone, and the saprolite zone [19].

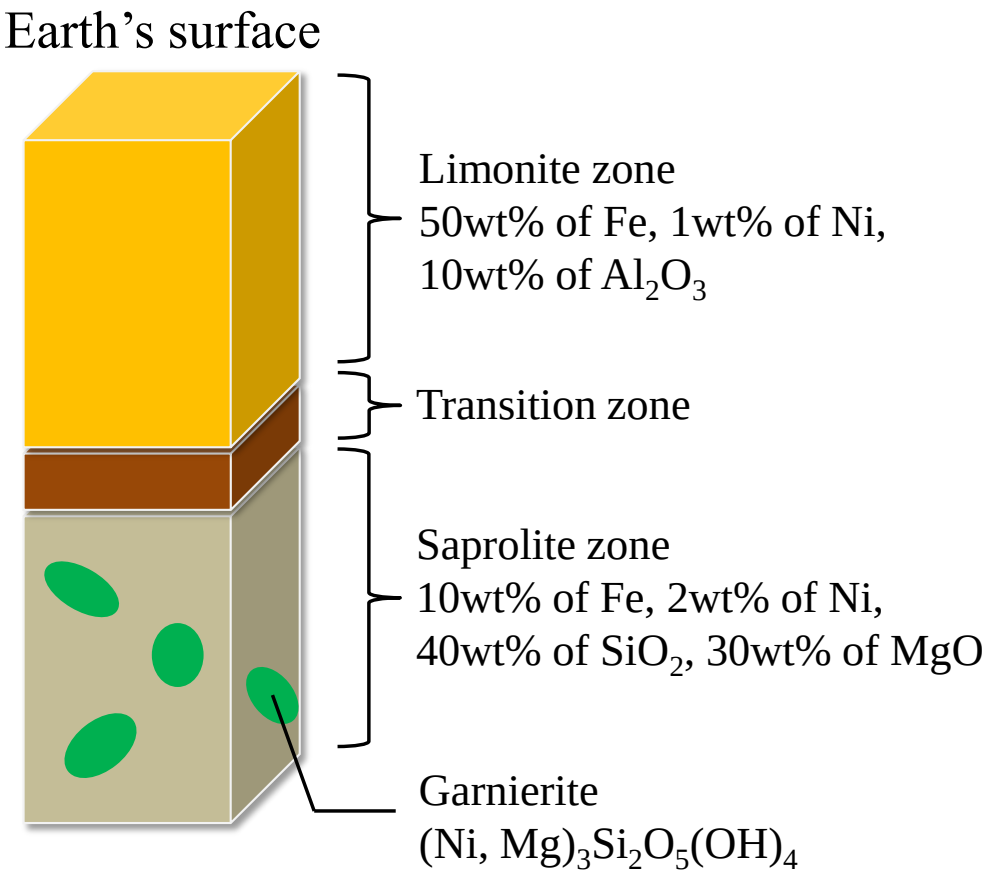

Figure 1-4 Schematic image of the laterite soil [19].

The limonite zone is located near the surface of the earth. It contains around 50wt% of Fe as a form of FeOOH and 1wt% of Ni. The limonite ore, containing FeOOH, becomes nanoporous via the dehydration equation (1-1) as was mentioned above. The obtained nanoporous limonite ore has a potential to be utilized as a catalyst because it naturally contains Ni which is active catalyst in a lot of chemical reactions.

1-3-2. Limonite ore utilization as a catalyst

The limonite ore (FeOOH containing 1wt% of Ni) which can be nanoporous after mild calcination has a potential as a catalyst for chemical reactions. A lot of studies have been conducted for limonite ore as the catalyst of a chemical reaction. Followings are the examples of limonite ore utilization as a catalyst in some chemical reactions.

In 1979, Kiyomiya et al. investigated the reduction reaction of nitrogen monoxide with ammonia, oxygen, sulfur dioxide, and steam on the pellet which was prepared from natural limonite ore (from Philippine) [20]. The pellet became porous (49-90 m^2/g) as a result of mild pre-calcination before the catalytic use. The limonite ore was durable for the reaction at least 100 h at 350℃.

Cubeiro et al. focused on Fischer-Tropsch (FT) reaction; Synthesis of carbon hydride from hydrogen and carbon monoxide [21]:

$$(2n+1)H_2 + nCO \rightarrow C_nH_{2n+2} + nH_2O \qquad (1\text{-}3)$$

They prepared limonite ore catalyst promoted by manganese nitrate and potassium carbonate. During catalytic tests for FT reaction, the iron in the limonite changed to magnetite and carbide and the carbide successfully worked as a catalyst for formation of alkenes.

Tsubouchi et al. decomposed ammonia on a pre-reduced limonite ore catalyst [22]. They reduced the limonite ore by hydrogen at 500℃ and got metallic iron phase. The pre-reduced limonite ore was used as a catalyst at 300-500℃ and almost of all the input ammonia was successfully decomposed to nitrogen at 500℃. The obtained limonite ore became nitride after the catalytic utilization.

1-3-3. Dry reforming reaction

The dry reforming reaction is attractive hydrogenation reaction from carbon dioxide and hydrocarbon.

$$C_mH_n + mCO_2 \rightarrow (n/2)H_2 + 2mCO \qquad (1\text{-}4)$$

When methane is used as hydrocarbon, the reaction becomes most simple,

$$CH_4 + CO_2 \rightarrow 2H_2 + 2CO \ (\Delta H = 247 \text{ kJ/mol}, \Delta G = 0 \text{ at } 643℃) \qquad (1\text{-}5)$$

where ΔH and ΔG mean the standard enthalpy change and the free Gibbs energy change of a reaction, respectively. This reaction is an endothermic one and occurs at high temperature. Akiyama et al. revealed that endothermic chemical reactions are appropriate for the recovery of high-temperature waste heat in the iron and steel industry

from the viewpoint of exergy [23]. In addition to good method for effective heat recovery, the dry reforming reaction contributes to reduction of CO_2 emission and hydrogen production. The dry reforming reaction is known as a catalytic reaction; noble metal-based catalysts, such as Pt, show very high catalytic activity in this reaction [24]. However, the noble metals are so expensive, that is why, comparatively cheaper Ni-based catalysts have been mainly investigated for this reaction [25].

1-3-4. Limonite ore as a catalyst for the dry reforming of methane

As is mentioned above, the dry reforming reaction can be utilized for hydrogen production with CO_2 elimination and high-temperature waste heat recovery in the steel and ironmaking industry. Limonite ore has more benefits as a catalyst than the conventional Ni-based catalysts.

Limonite ore has potentials to be used as a catalyst in the dry reforming of methane because it becomes nanoporous after mild calcination and contains Ni components which show high catalytic performance. Moreover, ore-based catalyst is much cheaper and produced via much more simple processes than the conventional Ni-based catalysts. Figure 1-5 shows comparison of production processes between conventional Ni/Al_2O_3 catalyst and limonite ore catalyst. Conventional Ni/Al_2O_3 catalyst is produced from Ni nitrate ($Ni(NO_3)_2 \cdot 6H_2O$) and support Al_2O_3. Ni nitrate is produced by nitric acid treatment of metallic Ni [26]. Ni sulfide ore is firstly pulverized and beneficiated, then

roasted in an oxygen atmosphere to remove iron component [27]. The obtained matte, mixture of Ni and Cu sulfide, is leached by $CuCl_2$ to give Ni solution [27]. After that, metallic Ni is obtained via electrowinning process [27]. $Al(OH)_3$ is generally used for the synthesis of Al_2O_3 [28]. $Al(OH)_3$ is synthesized via bayer method at around 250℃ from bauxite ore and NaOH and the obtained $Al(OH)_3$ is heat treated to generate support Al_2O_3 [29]. The Al_2O_3 support is put into the Ni nitrate aqueous solution and Ni/Al_2O_3 catalyst is obtained after drying, calcination, and activation. On the other hand, the limonite ore catalyst can be prepared via very simple processed; pulverization, mild caicination for removal of combined water, and activation.

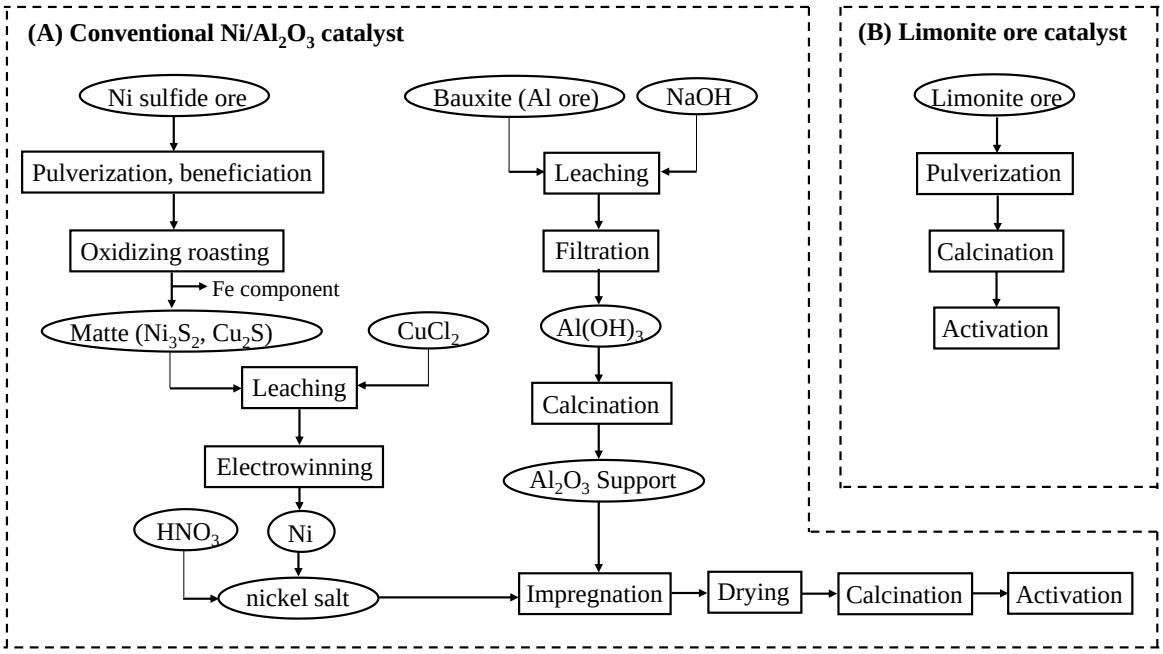

Figure 1-5 Comparison of catalyst production processes between (A): conventional catalyst and (B): limonite ore catalyst. Ni supported Al_2O_3 was chosen as conventional

catalyst.

Carbon deposition on the conventional Ni-based catalyst during usage for the dry reforming reaction causes catalytic deactivation. The Ni-based catalysts are less resistant to the carbon deactivation than the noble-metal-based catalysts [30]. The limonite ore catalysts, on the other hand, the can be recycled after carbon deactivation. The main component of the limonite ore catalyst is iron oxide; the deposited carbon can be worked as reductant of the iron oxide.

1-4. Goethite utilization as a carbon infiltrated material

1-4-1. Composites of iron ore and carbon-based materials

Blast furnace ironmaking, in which high-grade hematite ore or sinter ore, coke, and lime as raw materials, is the most common method to make metallic iron in the world. However, almost half of the CO_2 emissions in the iron and steel industry come from the blast furnace ironmaking processes including preparation processes of the raw materials. To utilize a method without coke oven and sintering processes the amounts of CO_2 emission and energy consumption in the iron and steel industry should be decreased. A lot of attempts have been tried to develop direct ironmaking method using carbon infiltrated iron ore.

Direct ironmaking method utilizes composite of iron ore and carbon material (carbon infiltrated iron ore) has been studied for coke-free ironmaking to reduce the CO_2 emissions in the iron and steel industry.

1-4-2. CVI Method to produce carbon infiltrated goethite ore

Carbon vapor infiltration (CVI) method have been studied to produce carbon infiltrated goethite ore (CVI ore) [31-40]. In the CVI process, carbonaceous materials containing heavy hydrocarbon such as coal and biomass are thermally decomposed to make tar vapor. Then the vapor infiltrates into the nanopores of goethite ore and

decomposes into carbon, gases, and light tar components. In 2009, Hata et al. succeeded to produce CVI ore containing 1.1—4.0mass% of carbon using biomass as a carbon source [31]. Then, the obtained ore was partially reduced to metallic iron at 900℃ [31].

Cahyono et al. then tried to utilize coal as a carbon source in the CVI process. They also observed the effects of carbon source and CVI temperature [32-36]. They used three kinds of carbon sources; high grade (bituminous) coal, low grade (lignite) coal, and biomass (palm kernel shell). They revealed coals released larger amount of tar vapor than biomass. The large amount of tar caused larger amount of deposited carbon in the CVI ore. The optimum CVI temperature was 600℃. Below 500℃, the rate of tar decomposition on the goethite ore was very slow. On the other hand, above 700℃, the rate of tar decomposition was fast, however, carbon gasification occurred and the amount of deposited carbon decreased. The highest carbon amount in the CVI ore was obtained at 600℃, the optimum temperature.

Distribution and morphology of the deposited carbon in CVI ore were also reported [37]. The deposited carbon was located only near the surface of the goethite ore and almost no carbon was detected in the center part. This is because the rate of carbon deposition might be much higher than that of infiltration of tar vapor into the ore-pores. As a result, carbon deposited near the surface occupied the pores and penetration of the tar vapor was blocked by the carbon. Observation of carbon morphology by Raman spectroscopy revealed that the deposited carbon was amorphous.

Hosokai et al. conducted kinetic analysis for reduction reaction of CVI ore [33]. They tried to use CVI ore produced from goethite ore and biomass, mixture of reagent Fe_3O_4 and carbon black, and mixture of reagent Fe_3O_4 and coke. Reduction started at around 1100℃ and 900℃ when Fe_3O_4/carbon black and Fe_3O_4/coke were used. The CVI ore, however, started to reduce at much lower temperature; approximately 700℃. The reduction at lower temperature was said to be the effect of close contact between goethite ore and carbon.

CVI ore is very attractive material for ironmaking because of the lower reduction temperature. As is mentioned above, a lot of study has been conducted to increase the amount of carbon in the CVI ore, however, only 5wt% is the maximum carbon content. This carbon amount is not enough for perfect reduction to metallic iron.

To overcome the defect of the CVI ore, carbon infiltrated goethite ore which is prepared from mixture of tar and goethite ore [41-43]. Maximum of 50 mass% of carbon is reachable in goethite ore by this method [43]. This carbon content is enough for the goethite ore to be reduced completely.

1-5. Purpose of this study

The iron and steel industry is one of the biggest industry in the world, however, the industry has three problems about resource, environment, and energy. The amount of utilization of high-grade iron ore has been increasing, resulting in degradation of the ore. The CO_2 emissions account for around 9% of the total emissions in the world. Large amount of high-temperature waste heat is emitted without effective utilization.

The goethite ore, one of the alternative iron ore in the iron and steel industry, contained 10% of combined water (CW). The CW in the goethite ore needs to be removed by calcination; this is disadvantage of the goethite usage because additional energy is essential for the calcination process. However, the goethite ore has an interesting property to become nanoporous material after mild calcination. This nanoporous goethite ore is promising as reaction field to solve the environmental and energetic problems in the iron and steel industry.

To solve the environmental and energetic problems in the iron and steel industry using this goethite-based ore, two solutions are proposed in this thesis: (1) Ni-containing goethite ore (limonite ore) as a catalyst for the dry reforming of methane and (2) fast combustion synthesis ironmaking of carbon infiltrated goethite ore.

This thesis consists of five chapters as follows:

Chapter 1 presents General Introduction of this study.

Chapter 2 and 3 describe observation of the catalytic performance of Ni-containing goethite-based ore (limonite ore) in the laterite soil. In chapter 2, some natural goethite-based ores including the limonite ores containing different amounts of Ni were utilized in the catalytic tests for the dry reforming of methane and their catalytic performances were compared. The effect of Ni in the ores was mainly discussed in this chapter.

In chapter 3, the detailed catalytic properties of the limonite ore were observed. The limonite ore contains a lot of Fe components and they easily change their composition (Fe_2O_3, Fe_3O_4, FeO, and Fe) during the catalytic tests. The state of the limonite ore was controlled during the catalytic properties were observed in detail in this chapter.

Chapter 4 describes fast ironmaking process, "combustion synthesis" using nanoporous goethite ore. Carbon-infiltrated goethite ore was synthesized from tar-based solution and mildly-calcined goethite ore and it was reduced by rapid heating in an oxygen atmosphere.

Theoretically possible conditions of the combustion synthesis reaction were mainly discussed from the viewpoint of the adiabatic temperature. Detailed calculations were taken place by a numerical software. The combustion synthesis ironmaking was experimentally conducted using carbon infiltrated goethite ore prepared via tar impregnation method. The reaction mechanism of the combustion synthesis reaction was mainly discussed here.

Chapter 5 presents the General conclusion of this thesis.

REFERENCES

[1] International Iron and Steel Institute, “Steel Statistical Yearbook”.

[2] International Monetary Fund, “Primary Commodity Prices”.

[3] International Energy Agency (IEA), “Coal Information”.

[4] USGS Minerals Yearbook.

[5] A.V. Todorut, D. Cirtina, L.M. Cirtina, Metalurgia 56 (2017).

[6] IEA, “CO_2 emissions from fuel combustion 2016”.

[7] IEA, “Tracking Industrial Energy Efficiency and CO_2 emissions” (2007).

[8] IEA, “Worldwide Trends in Energy Use and Efficiency, Key Insights from IEA Indicator Analysis”.

[9] T. Akiyama, J. Yagi, Tetsu-To-Hagane 82 (1996).

[10] G. Saito, T. Nomura, N. Sakaguchi, T. Akiyama, ISIJ International 56 (2016).

[11] F. Watari, J.V. Landuyt, P. Delavignette, S. Amelinckx, Journal of Solid State Chemistry 29 (1979).

[12] F. Watari, P. Delavignette, S. Amelinckx, Journal of Solid State Chemistry 29 (1979).

[13] F. Watari, P. Delavignette, J.V. Landuyt, S. Amelinckx, Journal of Solid State Chemistry 48 (1983).

[14] H. Naono, R. Fujiwara, Journal of Colloid and Interface Science 73 (1979).

[15] H. Naono, K. Nakai, T. Sueyoshi, H. Yagi, Journal of Colloid and Interface Science 120 (1987).

[16] J.L. Rendon, J. Cornejo, P. Arambarri, C.J. Serna, Journal of Colloid and Interface Science 92 (1983).

[17] JOGMEC 金属資源レポート 2013 最新選鉱技術事情鉱種別代表的プロセス編

[18] G.M. Mudd, Ore Geology Reviews 38 (2010).

[19] 辻 均, ロータリーキルンによるサプロライト Ni 鉱石の製錬における還元とリング付着のメカニズムに関する研究

[20] M. Kiyomiya, M. Kawai, Atmospheric environment 13 (1979) 559-561.

[21] M. L. Cubeiro, M.R. Goldwasser, M.J. Perez Zurita, C. Franco, F. Gonzalez-Jimenez, E, Jaimes, Hyperfine Interactions 93 (1994) 1831-1835.

[22] N. Tsubouchi, H. Hashimoto, Y. Otsuka, Catalysis Letters 105 (2005).

[23] T. Akiyama, K. Oikawa, T. Shimada, E. Kasai, J. Yagi, ISIJ International 40 (2000).

[24] M. Garcia-Dieguez, I.S. Pieta, M.C. Herrera, M.A. Larrubia, L.J. Alemany, Journal of Catalysts 270 (2010).

[25] D. Pakhare, J. Spivey, Chemical Society Review 22 (2014).

[26] 化学辞典、株式会社東京化学法人発行 (1999).

[27] K. Tozawa, Tetsu To Hagane 79 (1992).

[28] 触媒調製ハンドブック 株式会社エヌ・ティー・エス発行 (2011).

[29] F. Habashi, Hydrometallurgy 79 (2005).

[30] J.H. Kim, D.J. Suh, T.J. Park, K.L. Kim, Applied Catalysis A: General 197 (2000).

[31] Y. Hata, H. Purwanto, S. Hosokai, J. Hayashi, Y. Kashiwaya, and T.Akiyama, Energy & Fuels, 23(2), (2009), pp.1128-1131.

[32] A. N. Rozhan, R. B. Cahyono, N. Yasuda, T. Nomura, S. Hosokai, H. Purwanto, T. Akiyama, Energy and Fuels, 26 (2012), pp.7340-7346.

[33] S. Hosokai, K. Matsui, N. Okinaka, K. Ohno, M. Shimizu, and T. Akiyama, Energy Fuels, 26 (2012), pp. 7274–7279.

[34] R. B. Cahyono, A. N. Rozhan, N. Yasuda, T. Nomura, S. Hosokai, Y. Kashiwaya, T. Akiyama, Fuel Processing Technology 113, (2013), pp.84-89.

[35] R. B. Cahyono, A. N. Rozhan, N. Yasuda, T. Nomura, H. Purwanto, T. Akiyama, Energy Fuels 27 (2013), pp 2687–2692.

[36] R.B. Cahyono, N. Yasuda, T. Nomura, T. Akiyama, Fuel Processing Technology 119 (2014), pp. 272-277

[37] R. B. Cahyono, G. Saito, N. Yasuda, T. Nomura, and T. Akiyama, Energy Fuels, 2014, 28 (3), pp. 2129–2134

[38] R.B. Cahyono, N. Yasuda, T. Nomura, T. Akiyama, ISIJ International 55, No. 2 (2015), pp. 428-435.

[39] T. Nomura, R. B. Cahyono, T. Akiyama, Journal of Sustainable Metallurgy, 1

(2015), pp.115-125.

[40] A. Kurniawan, K. Abe, T. Nomura, and T. Akiyama, Energy Fuels, in press.

[41] Y. Mochizuki, N. Tsuboushi, T. Akiyama, Fuel Processing Technology 138 (2015).

[42] Y. Mochizuki, M. Nishio, N. Tsuboushi, T. Akiyama, Fuel Processing Technology 142 (2016).

[43] Y. Mochizuki, M. Nishio, J. Ma, N. Tsuboushi, T. Akiyama, Energy and Fuels 30 (2016).

Chapter 2

Limonitic Laterite Ore as a Catalyst for the Dry Reforming of Methane

2-1. Background

The steel industry has problems about high-temperature waste heat and CO_2 emission. Large amounts of high-temperature waste heat above 873 K from the steel industry, such as blast furnace slag and coke oven gas, are discharged without effective utilization [1]. Furthermore, CO_2 emission from the steel industry was estimated to account for approximately 15% of total emission in Japan [2]. The emission of high-temperature waste heat and CO_2 is not good for energy utilization and environment.

In an attempt to utilize high-temperature waste heat effectively and reduce CO_2 emission from the steel industry, we focused on the dry reforming reaction of methane, expressed below.

$$CH_4 + CO_2 \rightarrow 2H_2 + 2CO \quad (\Delta H° = +247 \text{ kJ mol}^{-1} \text{ at } 298 \text{ K}) \quad (2\text{-}1)$$

Akiyama et al. theoretically showed that the dry reforming reaction can occur using high-temperature waste heat and that thermal energy is converted to chemical energy in the production of H_2 and CO [3].[3] It is therefore an appropriate method for the utilization of high-temperature waste heat and reduction of CO_2 emission.

The dry reforming of methane is a catalytic reaction and a lot of metal-based catalysts, such as Ni [4-8], Co [8], Pt [9, 10], Rh [11], Ir [11], and Ru [12] have been investigated for use in the dry reforming reaction, with particular attention focused on Ni-based catalysts. These metal-based catalysts show good catalytic performance, however, they have some problems; (i) it is expensive because they consist of rare metals, (ii) metal particles on the catalysts should be nanosize and a lot of processes are needed such as impregnation, drying, and calcination, and (iii) when carbon is deposited on the surface of the catalysts, the catalytic performance decreases and they cannot be used anymore.

We focused on limonitic laterite ore as a catalyst for the dry reforming of methane. Limonitic laterite ore, which is abundant in South-east Asia and Oceania, is mainly composed of goethite (FeOOH). FeOOH can be easily dehydrated to form porous Fe_2O_3 (equation 1) which can then be used as a catalyst owing to its high surface area. Naono et al. reported that FeOOH decomposes into nanoporous Fe_2O_3 via dehydration when heated at approximately 573 K [13].

$$2FeOOH \rightarrow Fe_2O_3 + H_2O \qquad (2\text{-}2)$$

Limonitic laterite ore contains not only FeOOH but also Ni component which shows high catalytic performance for the dry-reforming reaction. The examples of the composition of limonitic laterite ores from Indonesia [14-17] and the Philippines [18-21] are shown in Table 2-1.

Table 2-1 Examples of the combpositions of limonite ores in laterite soil. Ore 1-4 and ore 5-8 are from Indonesian and the Philippine, respectively [14-21].

	Compositions (wt%)											
	T-Fe	NiO	Al_2O_3	SiO_2	CaO	MgO	MnO	Na_2O	TiO_2	Cr_2O_3	Co_3O_4	CW
Ore 1[19]	44.2-46.2	0.68-1.1	8.8-12.0	2.8-3.2	0.03	0.4-0.7	0.32-0.36	0.1-0.5	0.19-0.45	4.99-6.58	-	13.5-14.0
Ore 2[20]	50.9	0.38	8.8	9.7	0.03	0.3	-	-	-	5.90	0.03	11.0
Ore 3[21]	49.9	1.0	7.1	6.3	-	2.0	0.58	-	-	3.14	0.11	-
Ore 4[22]	41.0	1.2	6.5	12.6	0.3	4.7	0.82	-	-	2.86	0.12	13.2
Ore 5[23]	48.3	1.32	3.5	3.2	0.20	1.6	1.02	-	-	3.79	0.13	10.7
Ore 6[24]	40.5	2.0	8.5	9.2	0.0	1.7	2.8	0.0	-	2.3	0.3	-
Ore 7[25]	45.4	1.39	5.3	6.9	0.06	1.3	1.87	-	-	4.34	0.12	-
Ore 8[26]	37.0-39.7	0.72-1.11	5.7-6.1	2.6-3.2	0.02-0.03	0.0-0.2	0.12-0.43	0.0-0.1	0.06-0.14	1.24-2.25	0.06-0.08	-

*T-Fe and CW means total Fe and combined water.

Laterite ores contain approximately 1 wt% Ni and 10 wt% CW. That is why, limonitic laterite ore has a possibility to show good performance for the dry-reforming reaction.

In addition to the possibility as a catalyst, limonitic laterite ore has some good points compared with conventional metal-based catalysts; (i) limonitic laterite ore as a catalyst is much cheaper material since it is natural ore, (ii) it can be synthesized via more simple process (only dehydration) than conventional catalysts and limonitic laterite ore itself has nanostructure after dehydration, and (iii) limonitic laterite ore can be recycled as iron source after carbon deposition.

Carbon deposition on dehydrated nanoporous iron ore, on the other hand, have a good effect on the iron ore from the viewpoint of iron-making. Hata et al. deposited carbon on porous iron ore from pyrolyzed gas of biomass and obtained composite of carbon and partially reduced iron ore (Fe_3O_4) [22]. Hosokai et al. revealed that the composite shows faster reduction rate compared with mixture of reagent Fe_3O_4 and coke [23]. It is attractive to utilize nanoporous iron ore as a catalyst because they can be reused as iron resources after carbon deactivation.

In spite of their attracted characteristics, utilization of limonitic laterite ores as catalysts has not been reported, therefore, in this study, we investigated the catalytic properties of iron ores (laterite and non-laterite) containing different amounts of Ni for the dry-reforming reaction of methane and identified the effect of Ni in the limonitic laterite ore by examining its structure and comparing with non-Ni and Ni-supported iron ores. We also researched the porous structure, the degree of reduction, and the amount of carbon deposition of the iron ores.

2-2. Materials and experimental methods

2-2-1. Low grade iron ores

Four iron-ore-based catalysts, three of which were produced by dehydrating natural low-grade iron ores and the fourth was obtained by supporting Ni on the low-grade iron ore, were used for the catalytic tests. Table 2-2 shows the composition of the low-grade iron ores (LN, SN, and NN ores). LN (large amount of Ni) ore from Gaboc (Philippines), SN (small amount of Ni) ore from Sebuku (Indonesia), and NN (no nickel) ore from Hamersley (Australia) contain 1.18, 0.30, and 0 wt-%Ni, respectively. All iron ores contain crystal water so they can be dehydrated to produce porous materials.

Table 2-2. Compositions of the ores in this study.

	Compositions (wt%)										
	T-Fe	Ni	Cr_2O_3	Al_2O_3	SiO_2	CaO	MnO	MgO	TiO_2	Co	CW
LN ore	47.99	1.18	3.32	-	2.12	-	1.26	0.47	0.10	0.10	12.6
SN ore	50.88	0.30	5.90	8.84	9.66	0.03	-	0.31	-	0.03	11.0
NN ore	58.65	-	-	1.55	4.53	0.05	-	-	-	-	8.62

*T-Fe and CW means total Fe and combined water.

2-2-2. Preparation of low-grade iron ore catalysts

LN, SN, and NN ores were crushed to 300–1000 μm size and were dehydrated at 773 K for 4 h in a muffle furnace to afford natural iron ore catalysts. The Ni-supported iron ore (1.0 wt%Ni) was prepared from the NN ore and $Ni(NO_3)_2 \cdot 6H_2O$ aqueous solution to confirm the effect of nickel in the iron ores. The NN ore (before dehydration) was added to $Ni(NO_3)_2 \cdot 6H_2O$ aqueous solution and the solution was evaporated to dryness at 313 K (below the melting point of $Ni(NO_3)_2 \cdot 6H_2O$). After drying at 383 K under vacuum, it was then calcined at 773 K for 4 h.

2-2-3. Catalytic tests

Catalytic tests were performed in a catalytic packed-bed reactor. A schematic image of the equipment is shown in Figure 2-1. The input gases flowed through a quartz tube (φ6 mm × 554 mm) and passed over a catalytic zone containing an iron ore catalyst. The temperature of the catalytic zone was kept at a programmed temperature by a controlled system using a thermocouple which was placed just below the quartz wool to secure the iron ore catalysts.

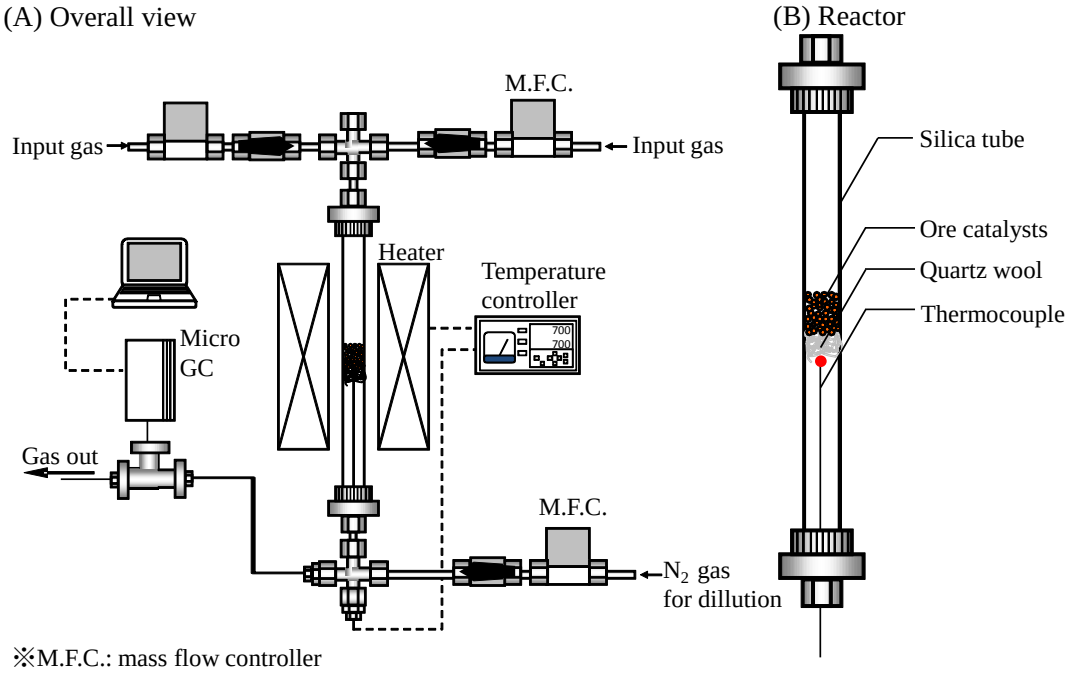

Figure 2-1 Schematic diagram of the apparatus for the catalytic tests.

First, we prepared dehydrated LN, SN, NN, and Ni-supported NN ores. Then, 1.0 g iron ore was placed in the quartz tube The iron ore was then heated to a target temperature (973–1173 K) at rate of 10 K/min under a N_2 flow. Just before the target temperature was reached, the N_2 flow was stopped and CH_4 and CO_2 flow began. The flow rates of the gases were controlled by mass flow controllers. The catalytic tests were performed for 1 h and the composition of the product gases was measured with a gas chromatograph (Agilent 3000, INFICON Co., Ltd., Yokohama, Japan) every 5 min. After the catalytic tests, the flow of CH_4 and CO_2 was stopped and N_2 was again flowed until the iron ore had cooled to room temperature.

2-2-4. Properties of the catalysts

Pore structure, phase identification, and surface observation measurements of the iron ores were conducted before and after the catalytic tests. The pore structure and surface area of the iron ores were estimated by gas adsorption measurements (Autosorb 6AG, Yuasa Ionics Co. Ltd., Osaka, Japan). Surface area was evaluated by the Brunauer-Emmett-Teller (BET) model and pore size distribution was calculated using the Barrett-Joyner-Halenda (BJH) method. Before and after the catalytic tests, the iron ores were analyzed using X-ray diffractometry (XRD; Miniflex, Rigaku, Tokyo, Japan), scanning electron microscopy (SEM; JSM-7001FA, JEOL, Tokyo, Japan), and transmission electron microscopy (TEM; JEM-2010F, JEOL, Tokyo, Japan) with energy dispersive X-ray spectroscopy (EDS). Carbon amount on the catalysts after catalytic tests were evaluated using a CHN/O/S elemental analyzer (CE-440; EAI, United States).

2-3. Results and discussion

2-3-1. Effect of surface area on the catalytic performance of the iron ores

Figure 2-2 shows the XRD patterns of the iron ores before and after dehydration. The results indicated that the iron ores mainly contained FeOOH (some Fe_2O_3 in SN and NN ores) before dehydration and Fe_2O_3 after dehydration. This meant that the decomposition reaction of CW ($2FeOOH \rightarrow Fe_2O_3 + H_2O$) occurred in all iron ores at 773 K.

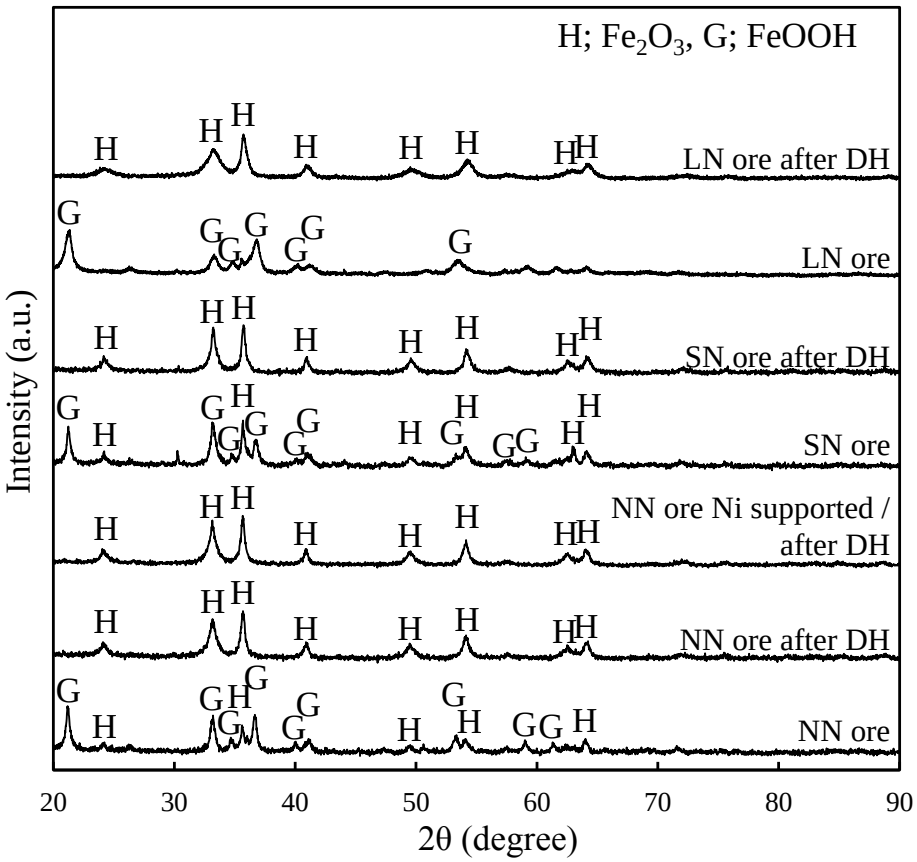

Figure 2-2 XRD patterns of the ores before and after dehydration at 773 K for 4 h.

Figure 2-3 shows the CO_2 conversion ratios of LN, SN, NN, and Ni-supported NN (1 wt% Ni) ores during the catalytic tests at 1173 K. The CO_2 conversion ratio is defined by the following equation:

$$CO_2 \text{conversion ratio} = \frac{\text{input flow rate of } CO_2 - \text{output flow rate of } CO_2}{\text{input flow rate of } CO_2} \quad (2\text{-}3)$$

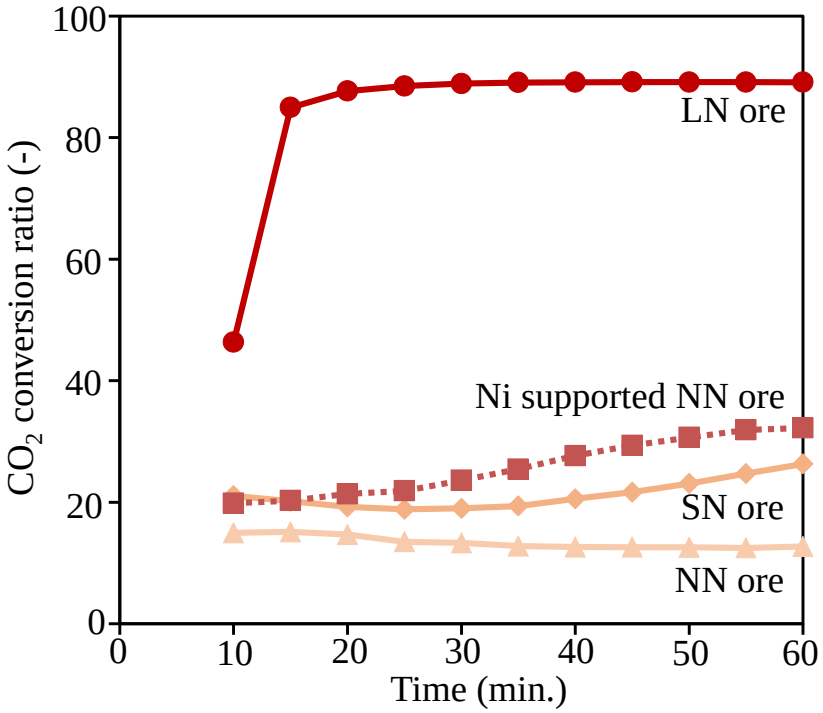

Figure 2-3 CO_2 conversion ratio ([input flow rate of CO_2 – output flow rate of CO_2]/input flow rate of CO_2) during the catalytic tests using LN, SN, NN, and Ni-supported NN ores at 1173 K for 1 h.

The LN ore had the highest CO_2 conversion ratio, followed by Ni-supported NN, SN, and NN ores. This order corresponds to the Ni content of the iron ores, with ores containing larger amounts of Ni showing higher CO_2 conversion ratios. However, the CO_2 conversion ratio of the LN ore was much higher than that of the Ni-supported NN ore, despite the fact that they contained almost the same amount of Ni.

Figure 2-4 shows the pore size distributions and BET surface areas of the iron ores before and after dehydration at 773 K for 4 h. Pores of 2–4 nm diameter were mainly formed during the dehydration process and all iron ores had higher surface areas (58.9–101 $m^2 g^{-1}$) after dehydration due to the formation of nanopores by detachment of CW.

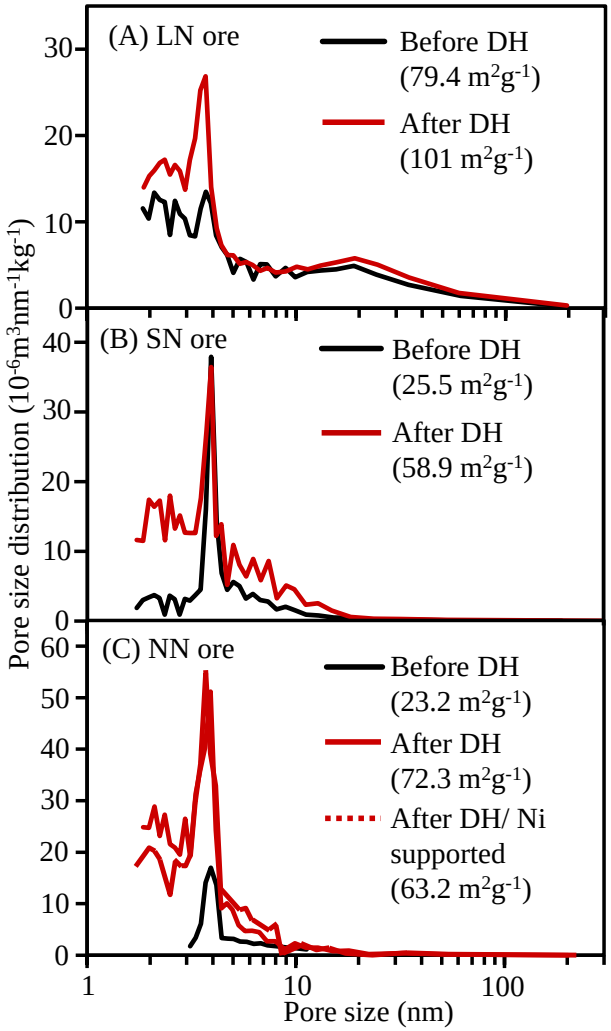

Figure 2-4 Pore size distributions and BET surface areas of the LN, SN, and NN ores before and after dehydration at 773 K for 4 h.

Figure 2-5 shows the SEM images of LN and SN ores before and after the dehydration process. The LN ore had a high surface area (79.4 $m^2\ g^{-1}$) even before dehydration as it contained many nanopores (layered structure, see SEM image (A) in Figure 2-5) and the

surface area increased further after dehydration (101 $m^2 g^{-1}$). The SN ore had a lower surface area (25.5 $m^2 g^{-1}$) than the LN ore before dehydration as it contained few nanopores (SEM image (C) in Figure 2-5). After dehydration, however, a lot of dot-like nanopores were observed in the SN ore. The BET surface area of the LN ore after dehydration (101 $m^2 g^{-1}$) was much higher than that of the Ni-supported NN ore after dehydration (63.2 $m^2 g^{-1}$), implying there was a possibility that better catalytic performance of LN ore was related to this higher surface area.

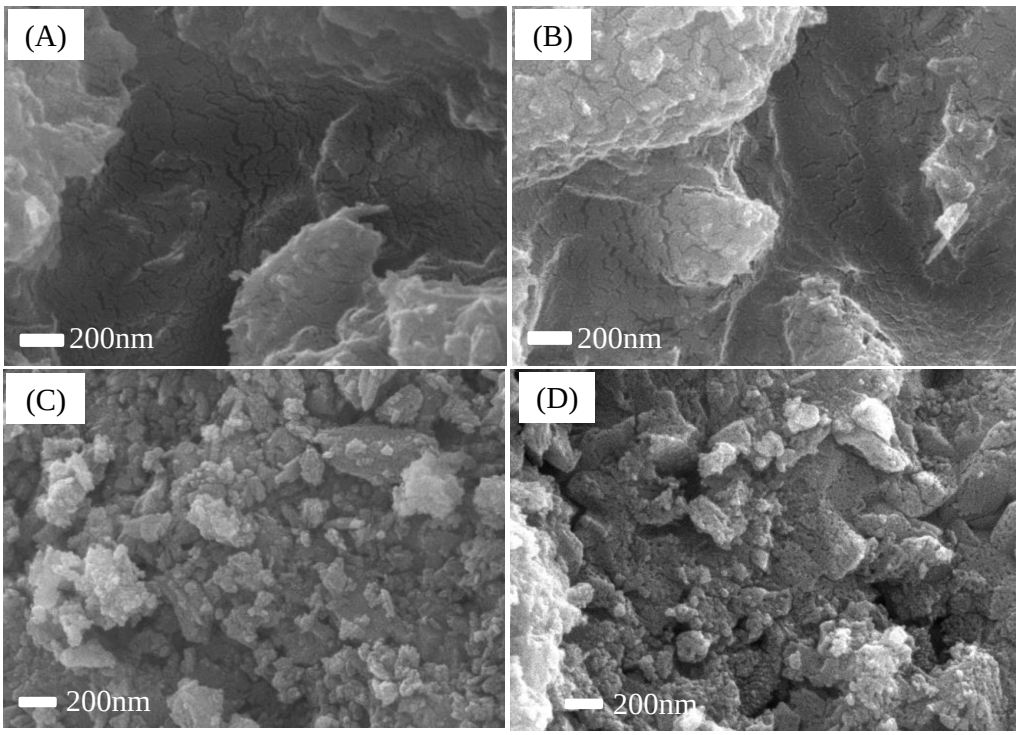

Figure 2-5 SEM images of (A); LN ore before dehydration (DH), (B); LN ore after DH, (C); SN ore before DH, and (D); SN ore after DH.

Fig. 2-6 shows the TEM images and EDS spectra of Ni-supported NN and LN ores before and after catalytic tests at 1173 K. We conducted EDS point analysis at certain points in these ores and found that Ni peaks could be detected everywhere in the LN ore, but only in a small part of the Ni-supported NN ore. This indicated that Ni existed as fine particles in the LN ore, but was of larger particle size (around 20 nm, Fig. 6) in the Ni-supported NN ore. According Tang and Valix, Ni exists as (Fe, Ni)O(OH) in iron matrix of laterite ores, meaning Ni disperses at the atomic level.[24] This higher dispersion means a higher surface area of Ni.

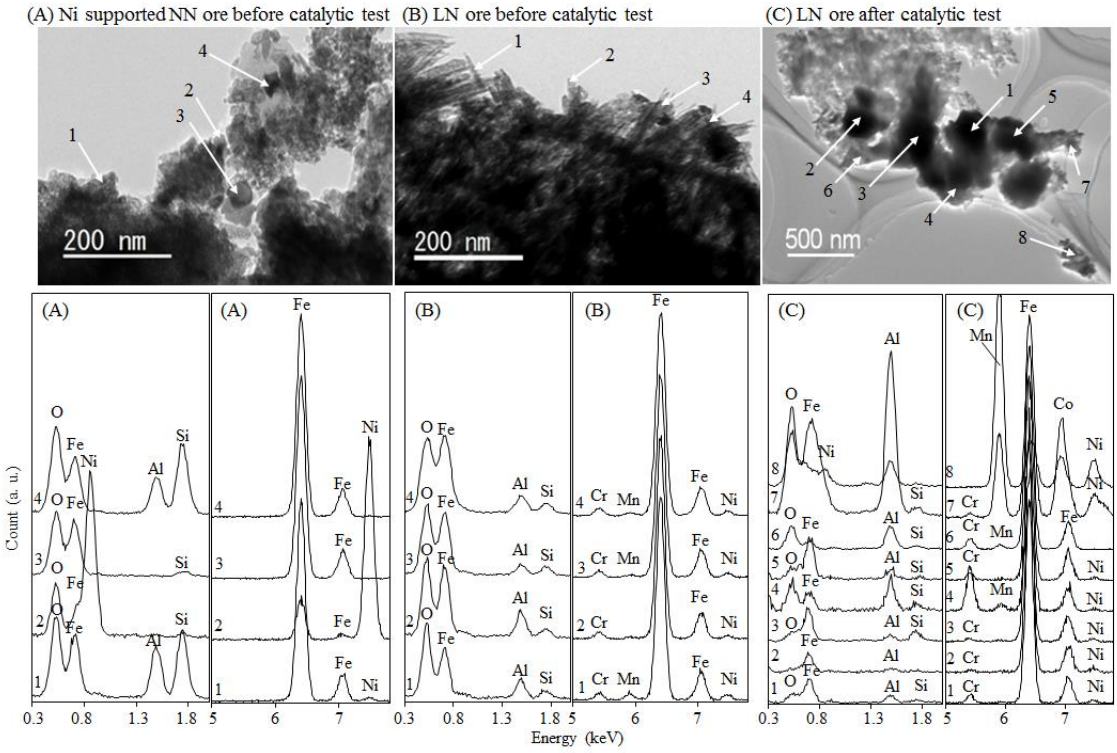

Figure 2-6 TEM images of (A); Ni-supported NN ore before the catalytic test, (B); LN ore before the catalytic test, and (C); LN ore after the catalytic test at 1173 K for 1 h, and EDS point analyses of each point in TEM images.

LN ore has higher surface area and higher Ni dispersion, resulting in the higher catalytic performance of the LN ore than that of the Ni-supported NN ore. Especially, higher Ni dispersion contributed more to higher catalytic performance because it is Ni to show good catalytic performance for the dry reforming reaction. After the catalytic test, some Ni was agglomerated in the LN ore but it still contained more highly dispersed Ni particles than the Ni-supported NN ore.

2-3-2. Catalytic performance of LN ore

Figure 2-7 shows the composition of CH_4, CO_2, H_2, and CO gas during the catalytic tests for LN ore. In the absence of catalyst, the dry-reforming reaction barely proceeded and the output gas contained little H_2 and CO. On the other hand, using LN ore as the catalyst, the decomposition of CO_2 and CH_4, and production of H_2 and CO increased. This indicated that LN ore has good catalytic properties for the dry reforming reaction. At higher temperatures, the amount of decomposed CO_2 and CH_4, and produced H_2 and CO increased further.

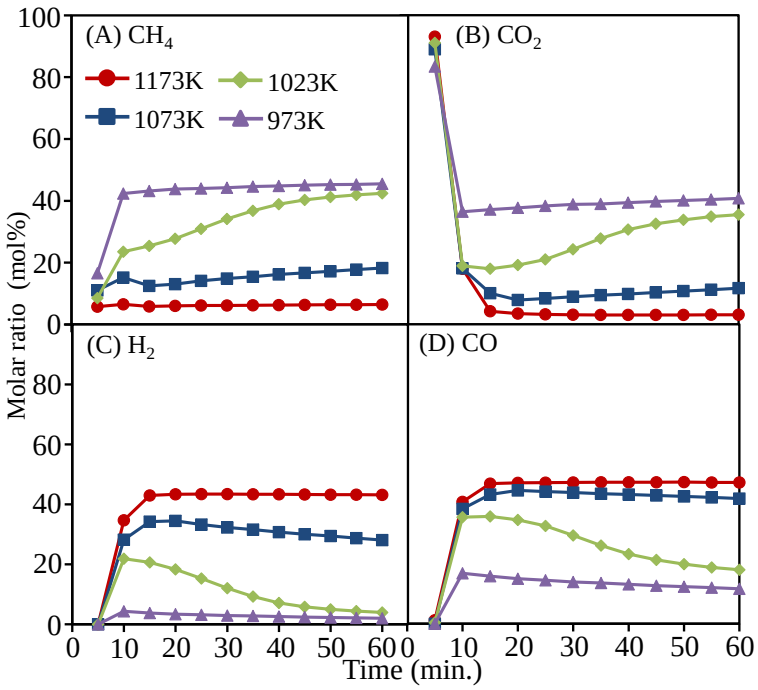

Figure 2-7 Gas composition of (A) CH_4, (B) CO_2, (C) H_2, and (D) CO during the catalytic tests using LN ore.

Figure 2-8 (A) shows the XRD patterns of the LN ore before and after the catalytic tests. Before the catalytic tests, iron existed as Fe_2O_3 (LN ore after DH in Figure 2-2). During the catalytic tests, Fe_2O_3 in the LN ore was reduced to Fe_3O_4, FeO, or Fe at all temperatures. Ni oxide in LN ore was also reduced at higher temperatures. Figure 2-8 (B) shows XRD patterns from 43 to 45 degrees. Ni content in LN ore was very small, that is why slower scanning speed was used for Figure 2-4 (B) to detect Ni components. Nickel existed as oxide during the catalytic tests at 973 and 1023 K and changed its form to metal at 1073 and 1123 K. The iron ore showed more reduction at higher temperatures and metallic iron and nickel were produced above 1073 K (reduction proceeded only to Fe_3O_4 at lower temperatures). The differences in the catalytic performance and reduction ratio of iron oxides at certain temperatures were evaluated as follows. At first, the dry reforming reaction rate increased with rising temperature and more reducing gases (H_2 and CO) were generated. Then, the reducing gases passed through the catalytic zone and reduced oxides, for instance, Fe and Ni oxides. These reduced metal components had even higher catalytic properties than oxides and much more reducing gases were produced. Low H_2/CO ratio at lower temperature was considered to be the effect of the reverse water gas shift reaction (RWGSR). The reaction equation of RWGSR is as follows:

$$H_2 + CO_2 \rightarrow CO + H_2O \quad (\Delta H° = +41 \text{ kJ mol}^{-1} \text{ at } 298 \text{ K}) \quad (2\text{-}4)$$

Some articles have reported that the dry reforming reaction and the RWGSR occurred at the same time at comparatively low temperature in case of using Ni catalysts [25, 26].

Figure 2-9 and Table 2-3 show the SEM images and BET surface area of the LN ore after the catalytic tests, respectively. Nanopores can be observed in the LN ore before the catalytic tests (SEM image (B) in Figure 2-5), but not after (Figure 2-9). The surface area of the LN ore drastically decreased after the catalytic tests, particularly at higher temperatures (101 and 4.20 $m^2 g^{-1}$ before and after catalytic tests at 1173 K, respectively). At higher temperature, LN ore had metal components (Fe and Ni) and they were more easily sintered than oxides.

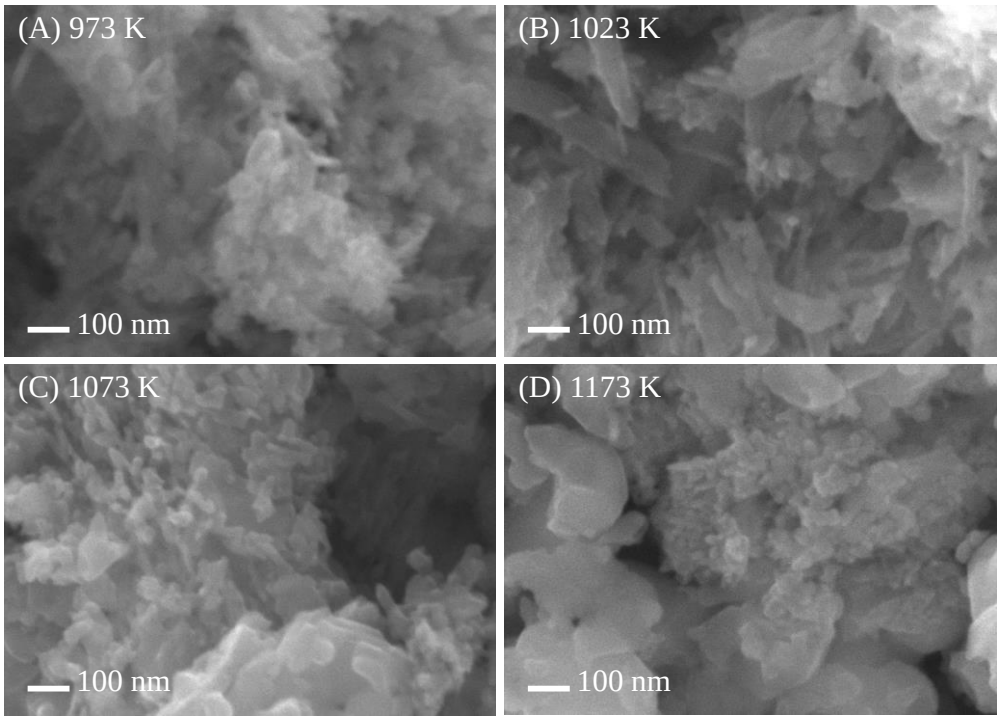

Figure 2-9 SEM images of LN ore after the catalytic tests at (A) 973 K, (B) 1023 K, (C) 1073 K, and (D) 1173 K.

Table 3. BET surface areas of LN ore before and after catalytic tests.

	LN ore before catalytic tests	LN ore after catalytic tests			
		973 K	1023 K	1073 K	1173 K
Surface area (m^2 g^{-1})	101	35.4	22.9	12.1	4.20

At all experimental conditions in this study, no carbon was detected on the iron-ore catalysts. The catalytic performance of limonitic laterite ore in this study was inferior as compared with that of Ni-based catalysts which was reported before. Ni shows high catalytic performance in the form of metallic Ni, so Ni-based catalysts are generally pre-reduced for several hours under flow of hydrogen before catalytic tests [4-8]. We did not conduct pre-reduction of iron-ore-catalyst because reduction of iron ore during the catalytic tests was one purpose in this study from the viewpoint of ironmaking using low-grade iron ores. It might be essential to conduct pre-reduction to improve the catalytic performance at lower temperatures.

2-4. Summary

We utilized Ni-containing low-grade iron ores (LN, SN, and NN ores) and Ni-supported low-grade iron ore (Ni-supported NN ore) as catalysts for the dry reforming reaction of methane ($CH_4 + CO_2 \rightarrow 2H_2 + 2CO$) by conducting catalytic tests under CH_4 and CO_2 flow (CH_4:CO_2 = 1:1) at 973–1173 K.

All iron ores were successfully dehydrated at 773 K for 4 h and FeOOH became Fe_2O_3. The CO_2 conversion ratio of the LN ore was much higher than that of Ni-supported NN ore despite the fact that they contained almost the same amount of Ni. This is due to higher surface area of the LN ore (101 $m^2\ g^{-1}$) than the Ni-supported NN ore (63.2 $m^2\ g^{-1}$) and higher dispersion of Ni in the LN ore. Ni existed quite finely in the LN ore, but had a much larger particle size in the Ni-supported NN ore. Smaller Ni particles have a higher surface area, resulting in the higher catalytic performance of the LN ore.

With LN ore as the catalyst, at higher temperatures the amount of decomposed CO_2 and CH_4, and produced H_2 and CO increased. The reduction of iron ores proceeded more at higher temperatures and metallic iron and nickel were produced above 1073 K; reduction did not progress past Fe_3O_4 at lower temperatures. This is due to the higher amounts of reducing gas (H_2 and CO) at higher temperatures.

This article demonstrated that Ni-containing low-grade iron ore could be utilized as

a catalyst for the dry reforming of methane. However, the catalytic property was inferior to another Ni-based catalysts and the dry reforming reaction requires high temperatures, which causes nanopores in the iron ore to disappear. It is therefore essential to conduct pre-reduction of low-grade iron ore for high catalytic performance at lower temperatures in order to take advantage of their high surface area.

REFERENCES

[1] Akiyama, T; Yagi, J., Tetsu-to-Hagane **1996**, 82, 177-184 (in Japanese).

[2] Gielen, D; Moriguchi, Y., Energy Policy **2002**, 30, 849-863.

[3] Akiyama, T; Oikawa, K; Shimada, T; Kasai, E; Yagi, J., ISIJ Int. **2000**, 40, 288-291.

[4] Wang, S; Lu, G.Q.M., Appl. Catal. B **1998**, 16, 269-277.

[5] Wang, S; Lu, G.Q.M., Appl. Catal. B **1998**, 19, 267-277.

[6] Wang, S; Lu, G.Q.M., Energy & Fuels **1998**, 12, 248-256.

[7] Montoya, J. A.; Romero-Pascual, E.; Gimon, C.; Del Angel, P.; Monzon, A., Catal. Today **2000**, 63, 71-85.

[8] Fan, M.S.; Abdullah, A.Z.; Bhatia, S., Appl. Catal. B **2010**, 100, 365-377.

[9] Damyanova, S.; Pawelec, B.; Arishtirova, K.; Martinez Huerta, M.V.; Fierro, J.L.G., Appl. Catal. B **2009**, 89, 149-159.

[10] Stagg-Williams, S. M.; Noronha, F. B.; Fendley, G.; Resasco, D. E., J. Catal. **2000**, 194, 240-249.

[11] Mark, M. F.; Maier, W. F., J. Catal. **1996**, 164, 122-130.

[12] Bradford, M. C. J.; Vannice, M. A., J. Catal. **1999**, 183, 69-75.

[13] Naono, H; Fujiwara, R J., Colloid and Interface Sci. **1980**, 73, 406-415.

[14] Fu, W.; Yang, J.; Yang, M.; Pang, B.; Liu, X.; Niu, H.; Huang, X., J. Asian Earth

Sci. **2014**, 93, 74-88.

[15] Purwanto, H.; Shimada, T.; Takahashi, R.; Yagi, J., ISIJ Int. **2002**, 42, 243-247.

[16] Wang, B.; Guo, Q.; Wei, G.; Zhang, P.; Qu, J.; Qi, T., Hydrometall. **2012**, 129-130, 7-13.

[17] Zhu, D.; Cui, Y.; Hapugoda, S.; Vining, K.; Pan, J., Trans. Nonferrous Met. Soc. China **2012**, 22, 907-916.

[18] Ma, B.; Wang, C.; Yang, W.; Chen, Y.; Yang, B., Int. J. Miner. Process. **2013**, 124, 42-49.

[19] Fan, R.; Gerson, A. R., Geochim. Cosmochim. Acta **2011**, 75, 6400-6415.

[20] Ogura, Y.; Murata, K.; Iwai, M., Chemical Geology **1987**, 60, 259-271.

[21] Andersen, J.; Rollinson, G. K.; Snook, B.; Herrington, R.; Fairhurst, R. J., Miner. Eng. **2009**, 22, 1119-1129.

[22] Hata, Y.; Purwanto, H.; Hosokai, S.; Hayashi, J.; Kashiwaya, Y.; Akiyama, T., Energy & Fuels **2009**, 23, 1128-1131.

[23] Hosokai, S.; Matsui, K.; Okinaka, N.; Ohno, K.; Shimizu, M.; Akiyama, T., Energy & Fuels **2012**, 26, 7274-7279.

[24] Tang, J. A.; Valix, M., Miner. Eng. **2006**, 19, 1274-1279.

[25] Barroso-Quiroga, M; Castro-Luna, A, Int. J. Hydrogen Energy **2010**, 35, 6052-6056.

[26] Baudouin, D; Rodemerck, U; Krumeich, F; Mallmann, A; Szeto, K; Menard, H; Veyre, L; Candy, J-P; Webb, P; Thieuleux, C; Coperet, C, J. Catal. **2013**, 297, 27-34.

Chapter 3

Effects of Reduction on the Catalytic Performance of Limonite Ore

3-1. Background

Unutilized high-temperature waste heat and CO_2 emissions are important issues in the steel industry. Significant amounts of high-temperature waste heat (> 600 °C) are emitted from blast furnaces, coke ovens, and converters without effective heat recovery [1]. The steel industry also emits large quantities of CO_2, which comprise around 15% of the total CO_2 emissions of Japan [2]. The dry reforming reaction of methane ($CH_4 + CO_2 \rightarrow 2H_2 + 2CO$; $\Delta H = 247$ kJ mol^{-1} at 298 K) is an effective method to produce energy in the form of hydrogen and carbon monoxide from carbon dioxide and waste heat [3].

The dry reforming reaction proceeds in the presence of metal based catalysts. Ni-based catalysts have been found to be one of the most effective catalysts for this reaction

[4–17]. Generally, Ni-based catalysts are prepared using a wet impregnation method from Ni nitrate solution with an oxide support. To improve the catalytic performance and stability of Ni-based catalysts, many studies have been performed. For example, alkali metals or alkaline earth metals have been added to the support materials to reduce the amount of carbon deposition and to improve catalytic stability [6–8]. Ni-containing oxides, such as perovskite and spinel compounds, exhibit strong interactions between the metal and its support [9–12]. Ni-based bimetallic catalysts have been also fabricated, and they exhibit high reactivity and stability [13–17].

In the present study, Ni-containing limonite ore was examined as a catalyst for the dry reforming reaction because of its simple preparation method, naturally occurring raw materials, low cost, and low resource utilization compared with previously reported Ni-based catalysts. Limonite ore requires only a simple dehydration process before it can be used as a catalyst. It is mainly composed of FeOOH, which is readily decomposed to porous Fe_2O_3 by heat treatment at 300–800 °C [18,19]. Limonite ore is naturally occurring and readily available. Therefore, it is significantly less expensive than commercially available catalysts. Generally, Ni-supported catalysts lose their catalytic activities by carbon deposition and cannot be used after deactivation, but limonite ore can be recycled into iron and nickel by reduction after catalyst deactivation.

Previously, we reported that Ni-containing limonite ore was an effective catalyst for the dry reforming reaction [20]. Ni-containing limonite ore exhibited the highest

catalytic activity of the three ore-based catalysts tested in the previous study (Ni-containing limonite ore, Ni-supported iron ore, and pristine iron ore). In this study, the effects of hydrogen reduction on the structure and catalytic performance of the Ni-containing limonite ore were examined in detail.

3-2. Materials and experimental methods

3-2-1. Preparation of the catalyst from limonite ore

Limonite ore (from Philippines) containing 1.18 wt% Ni, 47.98 wt% Fe, 0.14 wt% S, 2.12 wt% SiO_2, 1.26 wt% MnO, 0.47 wt% MgO, 0.10 wt% TiO_2, 3.32 wt% Cr_2O_3, 0.10 wt% Co_3O_4, and 12.6 wt% of combined water (CW) was used as a catalyst for the dry reforming reaction of methane. This limonite ore was crushed into 125–300 μm sized particles and heated to 500 °C at a heating rate of 5 °C min^{-1}; subsequently, it was calcined at this temperature for 4 h in air using a muffle furnace to remove any CW. These calcination conditions were enough for the complete dehydration of the limonite ore [20].

10 wt% Ni/Al_2O_3 catalyst as a reference was prepared by the following steps. α-Al_2O_3 reagent (35–50 μm, 99.0% up, Kanto Chemical Co., Inc., Tokyo, Japan) was added into $Ni(NO_3)_2 \cdot 6H_2O$ aqueous solution and the solution was evaporated at 80 °C. The obtained material was then calcined at 500 °C for 4 h in air.

3-2-2. Catalytic tests

The apparatus for the catalytic tests in this study was same as reported in detail elsewhere [20]. The dehydrated limonite ore was placed in a packed bed reactor consisting of a quartz tube (φ6 mm × 554 mm) and an infrared gold image furnace (RHL-

E410P, ADVANCE RIKO, Inc., Yokohama, Japan). The temperature of the furnace was measured using a thermocouple placed just below the catalyst and controlled with a temperature controller. The catalysts were placed in the quarts reactor. The amount of the limonite ore catalyst and the Ni/Al_2O_3 catalyst were 300 and 30 mg, respectively. Different amount of the catalysts was placed to set almost same Ni amount in the reactor. The length of the limonite ore catalyst bed was around 15 mm. In all the catalytic tests, the temperature of the catalyst region was maintained at 800–900°C for 6 h. Gases were flowed into the reactor from its top side, and their flow rates were controlled using mass flow controllers. The input gases, CH_4 (> 99.9%), CO_2 (> 99.99%), and H_2 (> 99.99999%), were diluted with Ar (> 99.999%). The total flow rate of the input gases was maintained at 30 L h^{-1} $g\text{-}_{catalyst}^{-1}$. The effects of hydrogen reduction on the catalytic performance of the limonitic laterite ore were determined using three different experiments (Figure 3-1).

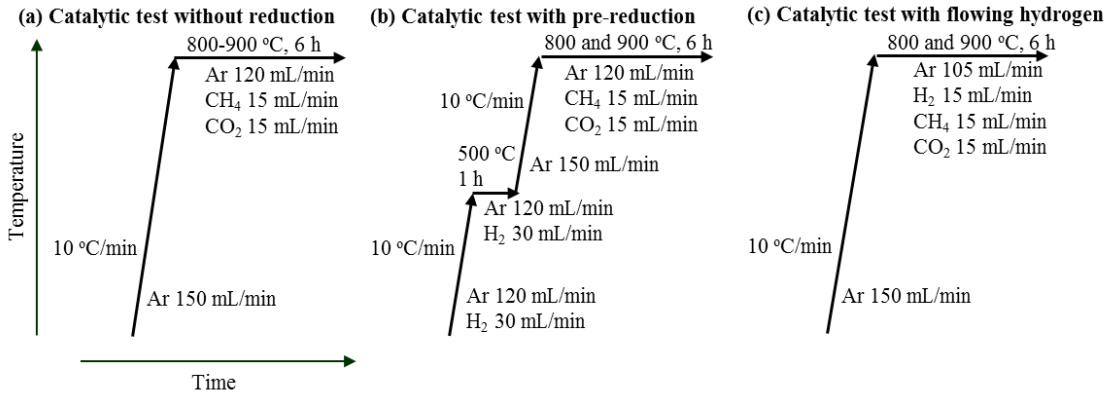

Figure 3-1 Three kinds of catalytic tests in this study.

3-2-2-1. Catalytic tests without pre-reduction (Figure 3-1, (A))

The limonite ore catalyst was heated to 800–900 °C at a heating rate of 10 °C min^{-1} in an Ar flow of 150 mL min^{-1}. Just before the target temperature was reached, Ar (120 mL min^{-1}), CH_4 (15 mL min^{-1}) and CO_2 (15 mL min^{-1}) were flowed over the catalyst. After that, the catalyst region was maintained at these conditions for 6 h.

3-2-2-2. Catalytic tests with pre-reduction (Figure 3-1, (B))

In this experiment, the limonite ore catalyst was reduced by hydrogen prior to the catalytic tests. The catalyst region was heated to 500 °C at a heating rate of 10 °C min^{-1} and maintained at 500 °C for 1 h while Ar (120 mL min^{-1}) and H_2 (30 mL min^{-1}) were flowed over the catalyst. After the reduction process was complete, the H_2 flow was stopped and the catalyst was heated to 800 or 900 °C at a rate of 10 °C min^{-1}. Just before the target temperature was reached, Ar (120 mL min^{-1}), CH_4 (15 mL min^{-1}), and CO_2 (15 mL min^{-1}) were flowed over the catalyst. After that, the catalyst region was maintained in this condition for 6 h.

3-2-2-3. Catalytic tests with hydrogen flow (Figure 3-1, (C))

The limonite ore catalyst was heated to 800–900 °C at a heating rate of 10 °C min^{-1} in an Ar flow (150 mL min^{-1}). Just before the target temperature was reached, Ar (105

mL min^{-1}), H_2 (15 mL min^{-1}), CH_4 (15 mL min^{-1}), and CO_2 (15 mL min^{-1}) were flowed over the catalyst. After that, the catalyst region was maintained in this condition for 6 h.

3-2-3. Characterization

In each catalytic test, the composition of the outflow gases was determined at 5 min interval using gas chromatography (Agilent 3000, INFICON Co., Ltd., Yokohama, Japan). Before and after the catalytic tests, phase identification and surface observation measurements of the limonite ore were conducted using X-ray diffractometry (XRD; Miniflex, Rigaku, Tokyo, Japan) and scanning electron microscopy (SEM; JSM-7001FA, JEOL, Tokyo, Japan) with energy dispersive X-ray spectroscopy (EDS). The specific surface area of the limonite ore was evaluated by N_2 gas adsorption measurements (Autosorb 6AG, Yuasa Ionics CO. Ltd., Osaka, Japan). Carbon formation on the catalysts was observed using a CHN/O/S elemental analyzer (CE-440; EAI, United States).

3-3. Results and discussion

3-3-1. Specific surface areas of the limonite ore catalysts

The specific surface areas of the limonite ore catalysts were evaluated by the Brunauer-Emmett-Teller (BET) model. Table 3-1 shows the BET surface area of the limonite ore before and after the catalytic tests.

Table 3-1. BET surface areas of the limonite ore catalysts before and after the catalytic tests.

	Before catalytic tests		Catalytic tests without pre-reduction			Catalytic tests with pre-reduction		Catalytic tests with flowing hydrogen	
	raw ore	after DH	800°C	850°C	900°C	800°C	900°C	800°C	900°C
BET surface area (m^2/g)	79.4	101.4	14.8	4.9	2.7	7.0	2.2	9.0	2.7

The BET surface area of the limonite ore catalyst before and after dehydration has been previously reported [20] and it was 79.4 m^2 g^{-1} before dehydration (DH) and 101.4 m^2 g^{-1} after DH at 500 °C. The limonite ore had cracks and it already had high surface area before DH. During DH, FeOOH was transformed into Fe_2O_3 by the following DH reaction and nano-sized pores formed [20], resulting in higher BET surface area after DH.

$$2FeOOH \rightarrow Fe_2O_3 + H_2O \qquad (3\text{-}1)$$

After the catalytic tests, the nanopores disappeared due to sintering and the surface areas of the limonite ores were significantly decreased at higher temperatures. Compared with the catalytic tests without pre-reduction, the decrease in the surface area was more significant after catalytic tests with pre-reduction and flowing hydrogen since the limonite ore had metallic phases which were easily sintered during the catalytic tests.

3-3-2. Catalytic tests with three different conditions

Before the catalytic tests, the condition of hydrogen reduction for the limonite ore was determined. The dehydrated limonite ore was heated up to 500 °C in H_2/Ar atmosphere (30 mL min^{-1} of H_2 and 120 mL min^{-1} of Ar). After heated, the limonite ore was maintained at this temperature for different holding times. Table 3-2 and Figure 3-2 show the weight decrease of the limonite ore at the different holding time and XRD patterns of the limonite ore gefore and after the hydrogen reduction.

Table 3-2. The amount of weight decrease of the limonite ore during hydrogen reduction.

Holding time (min.)	Weight decrease (%)
0	9.49
15	13.9
30	17.2
60	21.3
120	23.1
240	22.8
480	22.8

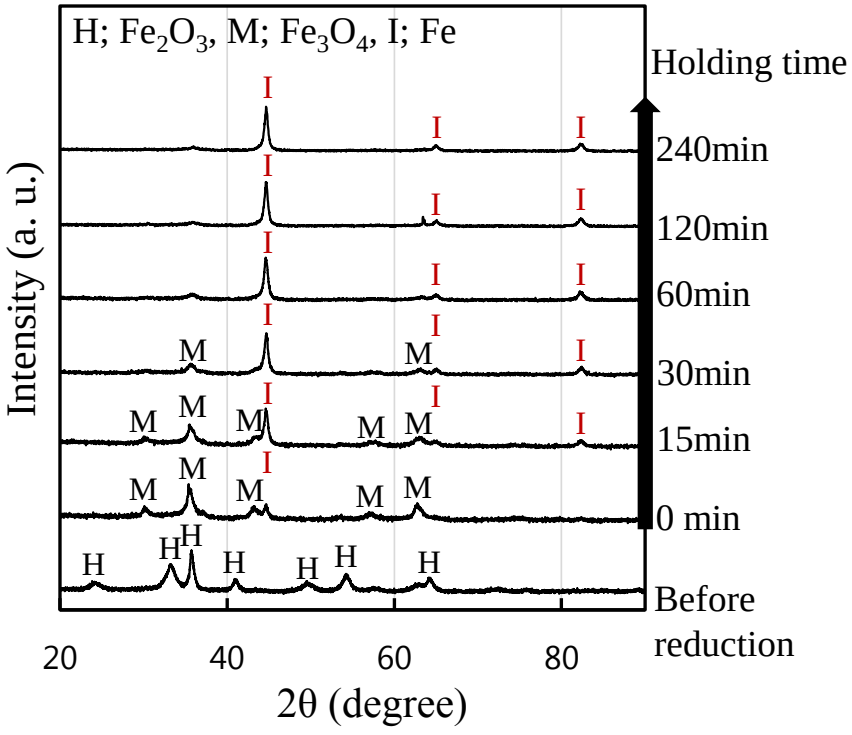

Figure 3-2. XRD patterns of the limonite ores before and after hydrogen reduction at

500 °C for different holding times.

The amount of weight decrease was higher at longer holding time, however, it did not change after 1 h holding. This meant 500 °C and 1 h reduction was enough for the limonite ore. XRD patterns also revealed that only iron peaks were obtained after holding of 1 h. That is why, the reduction condition of the limonite ore was determined to be at 500 °C for 1 h.

Figures. 3-3 and 3-4 show the consumption rates of the input CH_4 and CO_2 gases and the H_2/CO ratio in the output gas during the catalytic test without pre-reduction (Ar: CH_4: CO_2 = 8:1:1), with pre-reduction (Ar: CH_4: CO_2 = 8:1:1), and flowing hydrogen (Ar: H_2: CH_4: CO_2 = 7:1:1:1). The consumption rate of CH_4 and CO_2 was the highest in the catalytic test with flowing hydrogen, followed by the catalytic test without reduction and the catalytic test with pre-reduction.

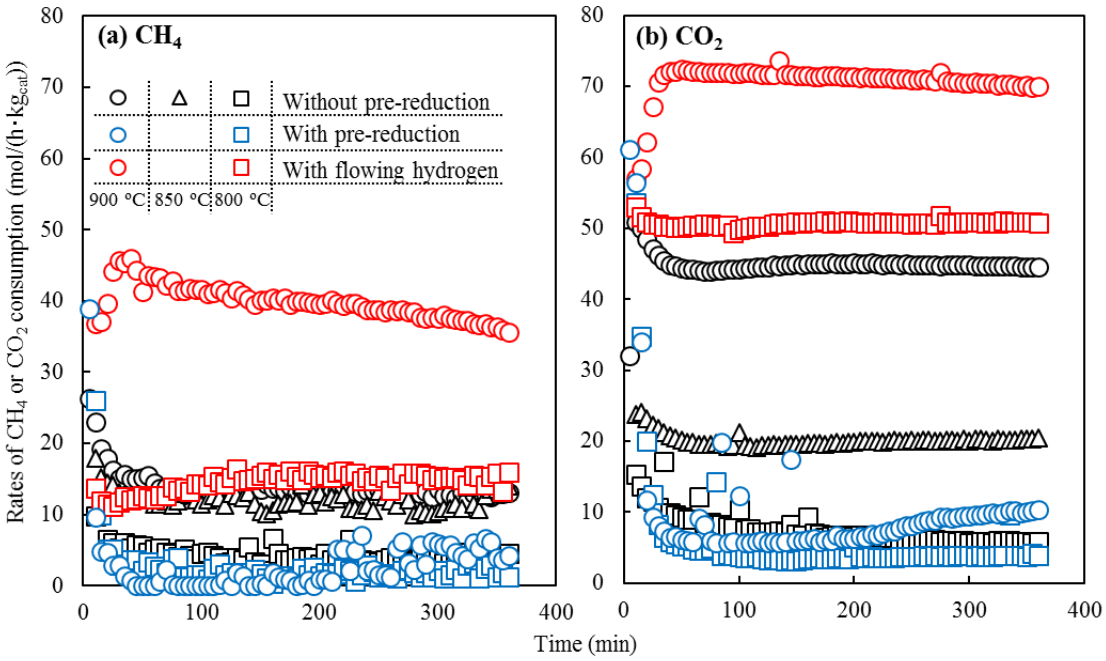

Figure 3-3 Rates of (a): CH_4 and (b): CO_2 consumption during the catalytic tests without reduction (black, Ar:CH_4:CO_2 = 8:1:1), the catalytic test with pre-reduction (blue, Ar:CH_4:CO_2 = 8:1:1), and the catalytic test with flowing hydrogen (red, Ar:H_2:CH_4:CO_2 = 7:1:1:1). The temperature was 800–900 °C and the gas flow rate was 30 L/(h·g_{cat}). The difference in the catalytic performances is likely related to the state of the limonite ore catalyst. Figure 3-5 (a) shows XRD patterns of the limonite ore catalysts before and after the catalytic tests and Figure 3-5 (b) shows the detailed XRD patterns of the catalysts after the catalytic tests with flowing hydrogen at 2θ = 44–45°.

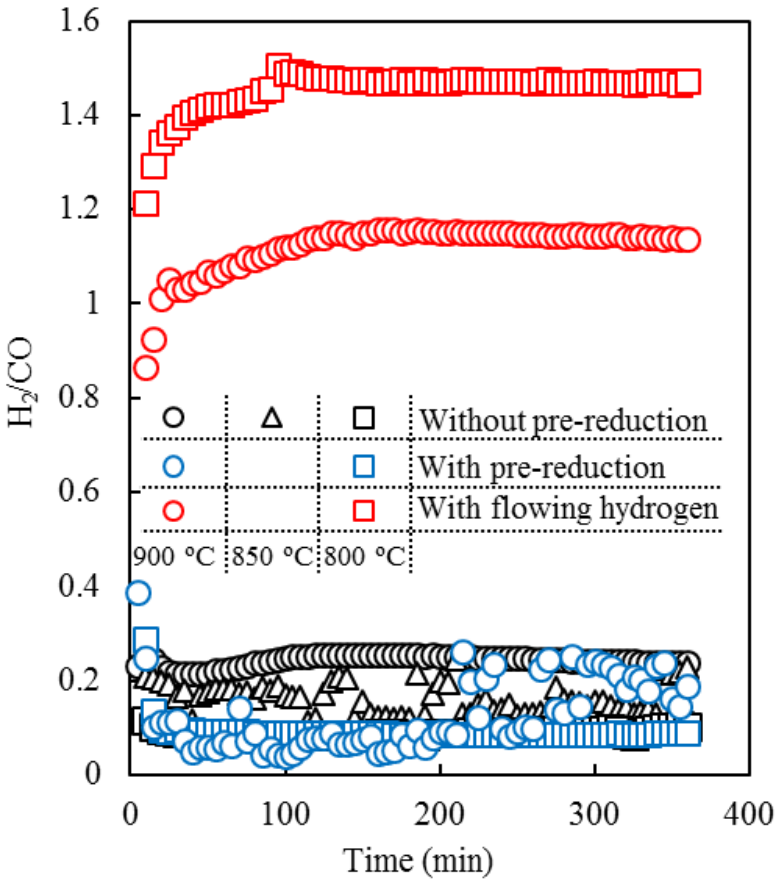

Figure 3-4. H_2/CO ratio in the output gases during the catalytic test without reduction (black, Ar:CH_4:CO_2 = 8:1:1), the catalytic test with pre-reduction (blue, Ar:CH_4:CO_2 = 8:1:1), and the catalytic test with flowing hydrogen (red, Ar:H_2:CH_4:CO_2 = 7:1:1:1). The temperature was 800–900 °C and the gas flow rate was 30 L/(h·g_{cat}).

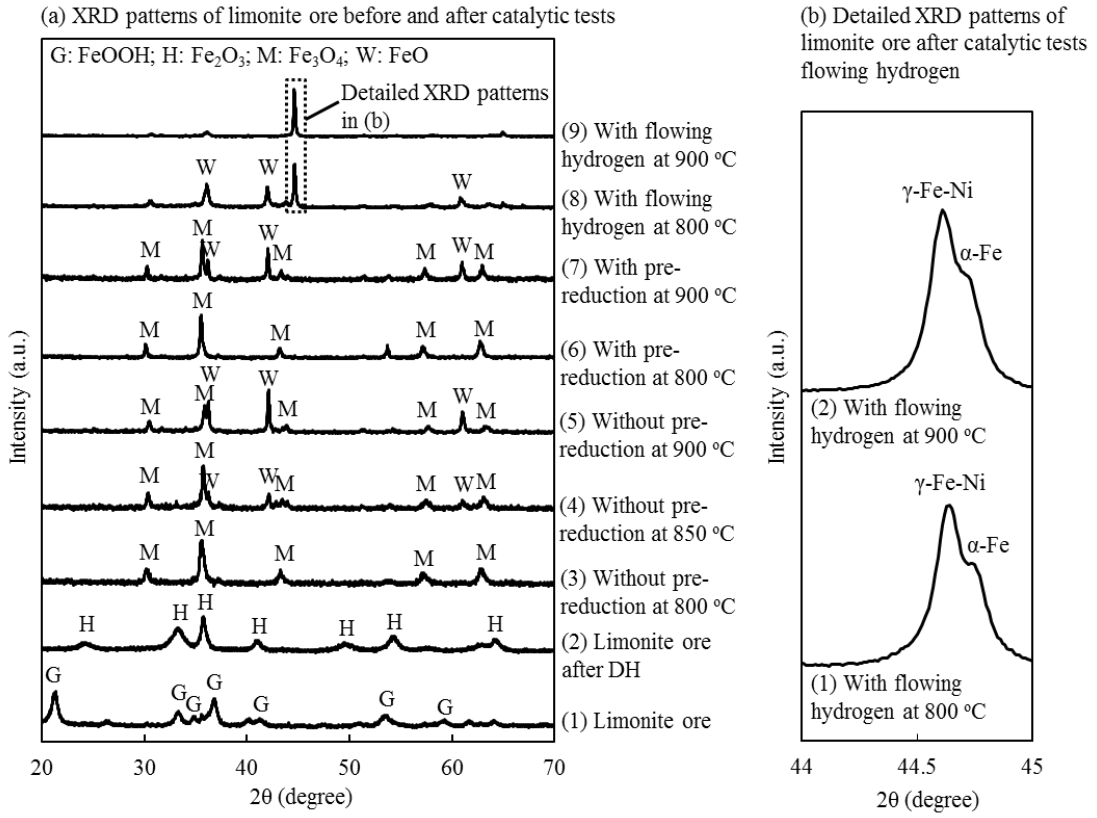

Figure 3-5 (a) XRD patterns of (1) limonite ore, (2) after DH, after the catalytic test at (3) 800 °C (4) 850 °C (5) 900 °C without reduction ($Ar:CH_4:CO_2$ = 8:1:1), after the catalytic test at (6) 800 °C and (7) 900 °C with pre-reduction ($Ar:CH_4:CO_2$ = 8:1:1), and after the catalytic test at (8) 800 °C and (9) 900 °C with flowing hydrogen ($Ar:H_2:CH_4:CO_2$ = 7:1:1:1). (b) Detailed XRD patterns of limonite ore after the catalytic test at (1) 800 °C and (2) 900 °C with flowing hydrogen ($Ar:H_2:CH_4:CO_2$ = 7:1:1:1). The total gas flow rate to the limonite ore catalyst was 30 L/(h·g_{cat}).

The bottom two lines in Figure 3-5 (a) represent the limonite ore before and after DH. It was confirmed that the dehydration reaction ($2FeOOH \rightarrow Fe_2O_3 + H_2O$) occurred completely after DH at 500 °C for 4 h. The other XRD patterns represent the limonite ore after the catalytic tests where Fe_3O_4 or FeO were dominant after the catalytic test without and with pre-reduction. Two separated peaks corresponding to Fe and Fe-Ni were observed at around $2\theta = 44.6°$ in Figure 3-5 (b). This can be explained by the Fe-Ni phase diagram produced by Cacciamani, et al. [21,22]. Fe and Ni comprise 48.0 and 1.2 wt% of the limonite ore, respectively, meaning the average mole fraction of Ni was 0.024 in the ore. At this mole fraction, it is reasonable that the two separated peaks are visible. During the catalytic tests, iron and nickel oxides were reduced to metallic iron and nickel by the input H_2 and formed bimetallic Fe-Ni. These Fe and Fe-Ni components worked better as a catalyst in the dry reforming reaction.

In the case of the catalytic tests with pre-reduction, the consumption rates were comparative to the other tests only at the beginning and then suddenly decreased as the catalytic test proceeded. Catalytic performance can generally be improved by pre-reduction, but the pre-reduction condition in this study did not improve the performance of the limonite catalyst. This is likely related to re-oxidation during the catalytic test. Fig. 3-6 shows the XRD patterns of the limonite ore catalysts after the catalytic tests with pre-reduction. The catalytic tests were performed at 900 °C for 15, 60, and 360 min. The bottom XRD pattern shows limonite ore catalyst after the pre-reduction, and just

before the catalytic test. The catalyst reduction to Fe and Fe-Ni after pre-reduction was confirmed, however, it was re-oxidized to Fe_3O_4 and FeO even after 15 min of the catalytic test. The Fe-Ni phase was lost by this re-oxidation and the catalytic performance of the limonite ore was significantly decreased. After that, the catalyst was additionally oxidized to a single phase of Fe_3O_4 at 60 min, then partially reduced to FeO at 360 min. The change in the catalytic performance around the 200-min mark (Fig. 3-3) may arise from the transformation of Fe_3O_4 to FeO. This would indicate that the catalytic performance of FeO is better than Fe_3O_4.

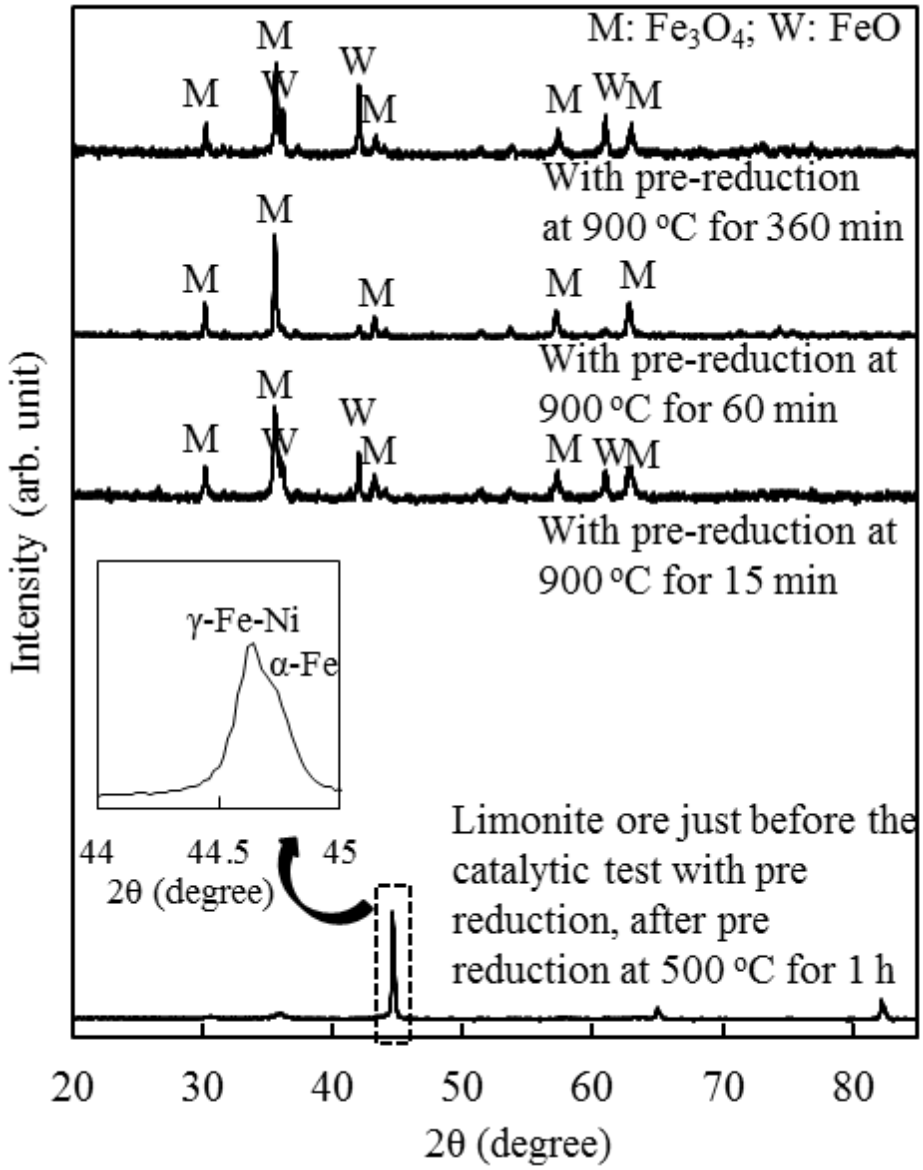

Figure 3-6. XRD patterns of limonite ore after the catalytic test with pre-reduction (Ar:CH_4:CO_2 = 8:1:1) at 900 °C for 15, 60, 360 min.

The consumption rates were always higher for the CO_2 than for CH_4. The H_2/CO ratios in the catalytic tests without and with pre-reduction were much lower than the one-to-one ratio theoretically expected (Fig. 3-4). This is because the product H_2 from the dry reforming reacted with the input CO_2 gas to produce CO and H_2O via the following reaction.

$$H_2 + CO_2 \leftrightarrow CO + H_2O \qquad (3\text{-}2)$$

H_2/CO ratio was the highest in the catalytic test flowing hydrogen, followed by the catalytic test without reduction and the catalytic test with pre-reduction. 10 vol% of H_2 was flowed during catalytic test with flowing hydrogen, that is why, the H_2/CO was much higher in the catalytic test with flowing hydrogen. The H_2/CO ratio was higher at high temperatures.

In this study, no carbon deposition was detected on the surface of the limonite ore after the catalytic tests. Carbon formation was less than 0.3 wt% in all of the experimental conditions.

3-3-3. Effects of Fe-Ni on the catalytic performance

Fig. 3-7 shows the SEM-EDS images of the limonite ores after catalytic tests with pre-reduction at 800 and 900 °C, and with flowing hydrogen at 900 °C. Significant Ni

segregation was observed in the limonite ore catalysts after the catalytic tests with pre-reduction at 800 and 900 °C. However, no segregation was observed after the catalytic test with flowing hydrogen at 900 °C, despite the higher reaction temperature. These results correspond well with those of Theofanidis et al [13]. Using elemental mapping of Fe/Ni after H_2 reduction and CO_2 oxidation at 850 °C, they found that Ni was homogeneously distributed in Fe-Ni reduced by H_2, and that Ni was separated from Fe in the Fe/Ni phase after oxidation by CO_2 [13]. The homogenous distribution of Ni resulted in a greater Ni surface area, which increased the catalytic activity of the limonite ore catalyst.

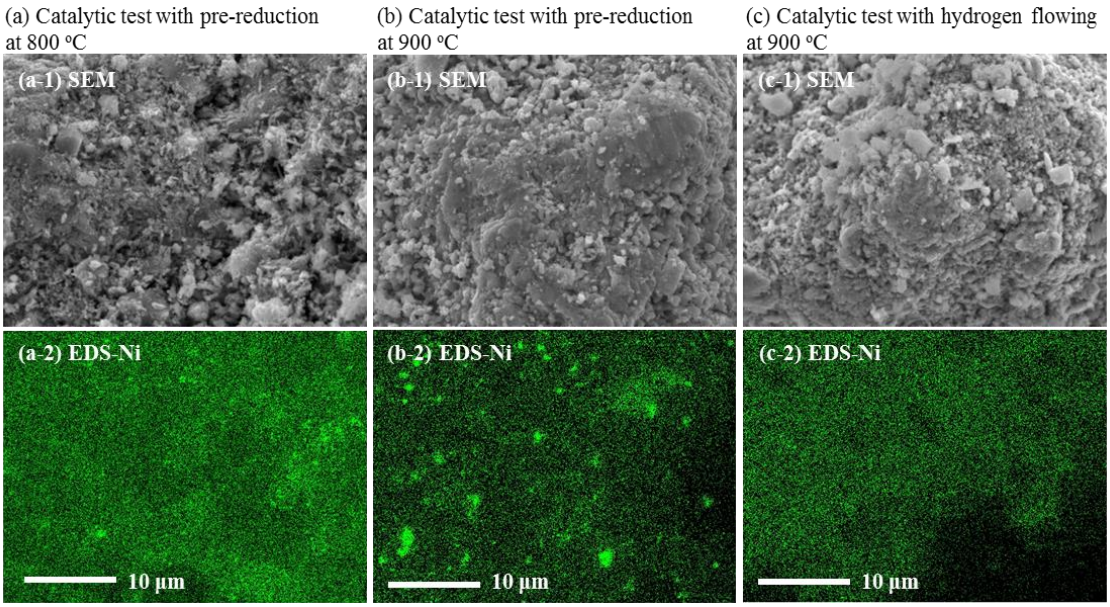

Figure 3-7. SEM (upper) and EDS (lower) images of the limonite ores after catalytic tests at 800 ºC (a-1 and a-2) and 900 ºC (b-1 and b-2) with pre-reduction and catalytic tests with flowing hydrogen at 900 ºC (c-1 and c-2).

Fig. 3-8 shows equilibrium diagram for Fe (Ni)-O-H and Fe (Ni)-O-C systems calculated using thermodynamic software. Reduction reactions of iron and nickel oxides by hydrogen and carbon monoxide were considered. The solid lines in the figure represent equilibrium of each reduction reaction by carbon monoxide and the dashed lines by hydrogen. Each line means equilibrium of two components lying next to each other. For example, the line of Eq. (1) in Fig. 3-8 represents that the hydrogen reduction of Fe_3O_4 to Fe achieves equilibrium. Judging from the diagram, the reduction reaction of NiO can occur at lower CO and H_2 concentration than the reduction reaction of Fe_3O_4 to FeO. That is why, existence of FeO implied that Ni was maintained as metal during the catalytic tests at 900 °C. The limonite ore has been Fe_3O_4/FeO/Ni during the catalytic test with pre-reduction at 900 °C and metallic Ni could not dissolve in the iron oxides, resulting in the significant segregation of Ni. It is important for limonite ores as a catalyst in the dry reforming reaction to maintain Fe-Ni phase during its catalytic utilization.

The catalytic activity of Ni-containing limonite ore depends upon its state. The presence of the Fe-Ni phase increases the catalytic activity, because it increased the surface area of Ni in the limonite ore. Therefore, reducing the flow rate of the input gases or increasing the length of the catalytic bed increases the efficiency the limonite ore catalysts, because the oxidation of the Fe-Ni phase is reduced.

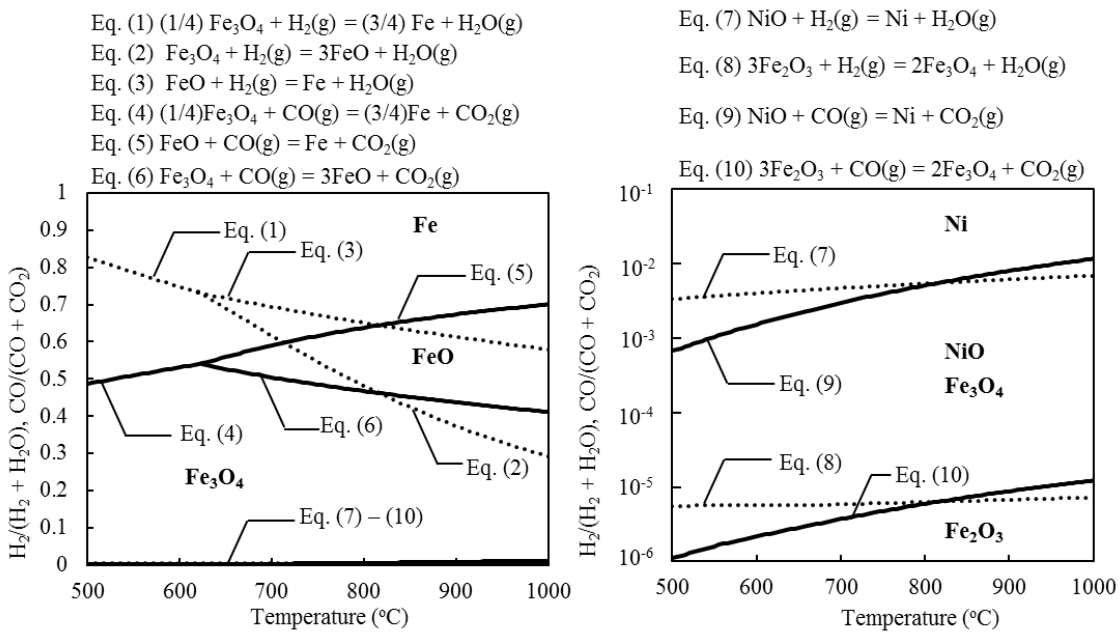

Figure 3-8. Equilibrium diagrams for (a) Fe (Ni)-O-H and (b) Fe (Ni)-O-C systems calculated using thermodynamic software. The considered iron and nickel components were Fe_2O_3, Fe_3O_4, FeO, Fe, NiO, and Ni.

3-3-4. Comparison of the limonite ore and Ni/Al_2O_3 catalysts

Fig. 3-9 (a) shows the CH_4 consumption rates on the limonite ore catalyst and the 10 wt% Ni/Al_2O_3 catalyst. The obtained consumption rates were normalized by the Ni amount in these catalysts. Conventional Ni/Al_2O_3 catalyst showed higher catalytic performance than the limonite ore catalyst. The catalytic performance in the dry reforming reaction depends strongly on its support and Al_2O_3 is comparatively good among oxide supports for Ni [23,24]. Takano et al. reported that the dry reforming reaction mainly occurs at the interface between metal and its support [25]. The limonite

ore contains small amount (2.12 wt% SiO_2, 1.26 wt% MnO, 0.47 wt% MgO, 0.10 wt% TiO_2, 3.32 wt% Cr_2O_3) of stable oxides. Among these oxides, for example, SiO_2 and TiO_2 are poorer supports for Ni-based catalysts compared with Al_2O_3 support [24]. That is why, there was less effect of support in the limonite ore catalyst, resulting in lower catalytic performance than that of the Ni/Al_2O_3 catalyst. However, the catalytic stability was better in the limonite ore. The catalytic performance continued to drop in the Ni/Al_2O_3 and 10% decrease in the CH_4 consumption rate was observed after 6 h experiment. On the other hand, although the limonite ore showed less performance, it was more stable during catalytic use.

In addition, the limonite ore should be much superior in terms of cost to produce the catalyst. We conducted cost benefit analysis for the catalysts and the results were shown in Fig. 3-9 (b). Cost benefit performance (CBP), which were used for this analysis, was defined by the following equation;

CBP = (Performance of the catalyst)/(Catalyst production cost)

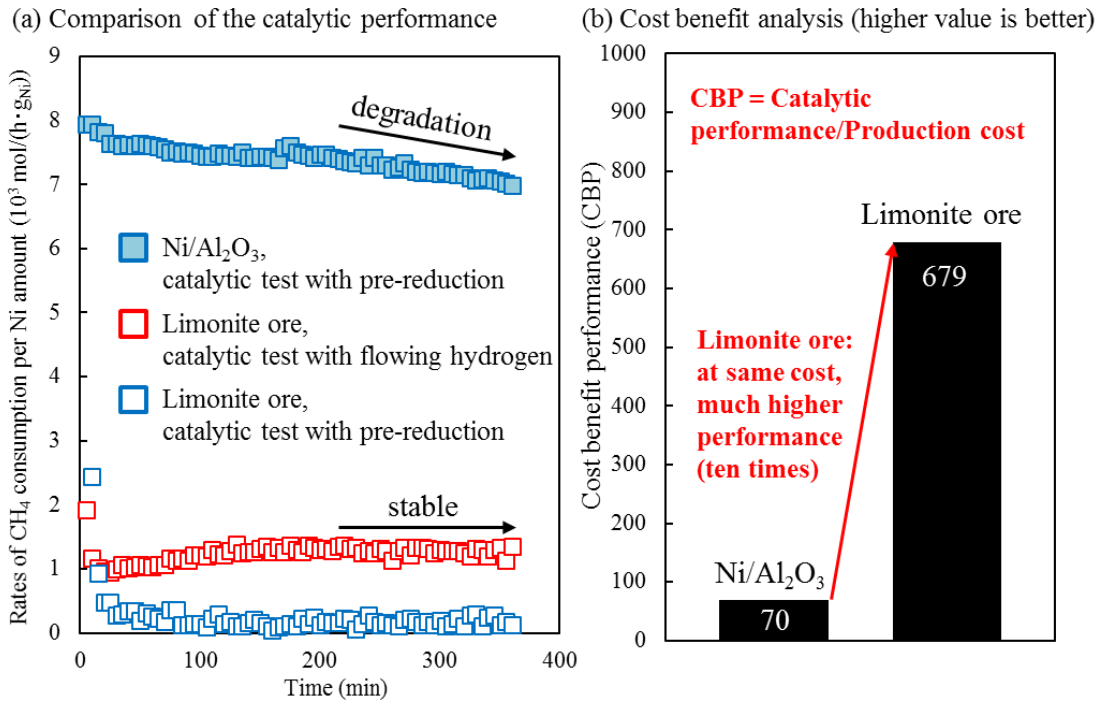

Figure 3-9. (a) Rates of CH_4 consumption (normalized by the Ni amount in the catalysts) on the Ni/Al_2O_3 and limonite ore catalysts during the catalytic tests with pre-reduction ($Ar:CH_4:CO_2$ = 8:1:1) and the catalytic test with flowing hydrogen ($Ar:H_2:CH_4:CO_2$ = 7:1:1:1) at 800 ℃. (b) Cost benefit analysis for the limonite ore and the Ni/Al_2O_3. Cost benefit performance (CBP) (= Performance of the catalyst (CH_4 consumption rate)/Catalyst production cost) was used to conduct the analysis.

In this study, the performance of the catalyst meant the rate of CH_4 consumption (mol h^{-1} $kg_{catalyst}^{-1}$). The costs of the limonite ore (1.5 wt%Ni) and industrial catalysts without rare metal are said to be 0.023-0.024 $/kg [26] and 100 $/kg [27]. These prices

were used for the analysis. From the definition, higher CBP means it is better catalyst. The limonite ore showed ten times larger CBP as the Ni/Al_2O_3. The limonite ore was much better catalyst taking into account the production cost.

3-3-4. Summary

In this study, the catalytic activity of Ni-containing limonite ore in the dry reforming reaction ($CH_4 + CO_2 \rightarrow 2H_2 + 2CO$) was evaluated in catalytic tests without pre-reduction, with pre-reduction, and with flowing hydrogen.

During dehydration, FeOOH in the limonite ore perfectly transformed into Fe_2O_3 and the surface area of the limonite ore got higher because nanopores were introduced in the limonite ores. The surface area drastically decreased after the catalytic tests because the nanopores were eliminated more at higher temperatures due to sintering.

The three kinds of catalytic tests revealed that the catalytic performance of the limonite ore depended on the iron phase. In this study, the phase of iron in the limonite ore changed to oxides (Fe_3O_4 and FeO) and metals (Fe and Fe-Ni). When the iron mainly existed as oxides, the catalytic performance of the FeO was better than that of Fe_3O_4. Fe and Fe-Ni showed much greater catalytic performance than the oxides.

The iron phases in the limonite ore significantly affected Ni surface area. When iron oxides were the main phase, Ni segregated during the catalytic tests, resulting in lower Ni surface area and lower catalytic activity. When the reduction proceeded to metallic iron, bimetallic Fe-Ni generated and Ni could exist homogeneously in the Fe-Ni phase, resulting in higher Ni surface area and higher catalytic activity.

REFERENCES

[1] T. Akiyama, J. Yagi, Tetsu to Hagane 82 (1996) 177–184 (in Japanese).

[2] D. Gielen, Y. Moriguchi, Energy Policy 30 (2002) 849–863.

[3] T. Akiyama, K. Oikawa, T. Shimada, E. Kasai, J. Yagi, ISIJ Int. 40 (2000) 288–291.

[4] S. Wang, G.Q.M. Lu, Appl. Catal., B 16 (1998) 269–277.

[5] J. A. Montoya, E. Romero-Pascual, C. Gimon, P. Del Angel, A. Monzon, Catal. Today 63 (2000) 71–85.

[6] M. Barroso-Quiroga, A. Castro-Luna, Int. J. Hydrogen Energy 35 (2010) 6052–6056.

[7] T. Horiuchi, K. Sakuma, T, Fukui, Y. Kubo, T. Osaki, T. Mori, Appl. Catal., A 144 (1996) 111–120.

[8] Z. Alipour, M. Rezaei, F. Meshkani, J. Ind. Eng. Chem. 20 (2014) 2858–2863.

[9] G. Gallego, C. Batiot-Dupeyrat, J. Barrault, E. Florez, F. Mondragon, Appl. Catal., A 334 (2008) 251–258.

[10] K. Sutthiumporn, T. Maneerung, Y. Kathiraser, S. Kawi, Int. J. Hydrogen Energy 37 (2012) 11195–11207.

[11] L. Zhou, L. Li, N. Wei, J. Li, J. Basset, ChemCatChem 7 (2015) 2508–2516.

[12] N. Sahli, C. Petit, A.C. Roger, A. Kiennemann, S. Libs, M.M. Bettahar, Catal. Today 113 (2006) 187–193.

[13] S. Theofanidis, V. Galvita, H. Poelman, G. Marin, ACS Catal. 5 (2015) 3028–

3039.

[14] K. Ray, S. Sengupta, G. Deo, Fuel Process. Technol. 156 (2017) 195–203.

[15] J. Zhang, H. Wang, A. Dalai, J. Catal. 249 (2007) 300–310.

[16] S. Theofanidis, R. Batchu, V. Galvita, H. Poelman, G. Marin, Appl. Catal., B 185 (2016) 42–55.

[17] Z. Huang, H. Jiang, F. He, D. Chen, G. Wei, K. Zhao, A. Zheng, Y. Feng, Z. Zhao, H. Li, J. Energy Chem. 25 (2016) 62–70.

[18] H. Naono; R J. Fujiwara, Colloid Interf. Sci. 73 (1980) 406–415.

[19] G. Saito, T. Nomura, N. Sakaguchi, T. Akiyama, ISIJ Int. 56 (2016) 1598–1605.

[20] K. Abe, G. Saito, T. Nomura, T. Akiyama, Energy Fuels 30 (2016) 8457–8462.

[21] G. Caccimani, A. Dinsdale, M. Palumbo, A. Pasturel, Intermet. 18 (2010) 1148–1162.

[22] G. Caccimani, J. De Keyzer, R. Ferro, U.E. Klotz, J. Lacaze, P. Wollants, Intermet. 14 (2006) 1312–1325.

[23] A. Takano, T. Tagawa, S. Goto, J. Chem. Eng. Japan 27 (1994) 727–731.

[24] H.M. Swaan, V.C.H. Kroll, G.A. Martin, C. Mirodatos, Catal. Today 21 (1994) 571–578.

[25] A. Takano, T. Tagawa, S. Goto, Kagaku Kougaku Ronbunsyu 21 (1995) 1154–1160 (in Japanese).

[26] Base Metals News, https://www.fastmarkets.com/base-metals-news/asia/2016-review-china-imports-philippine-laterite-ore-hit-year-denr-audit-125904/ (accessed 14 September 2017).

[27] M. Iwamoto, M. Akita, M. Onaka, T. Tanaka, T. Deguchi, K. Tomishige, H. Yamashita, I. Yamanaka (2011) “How to Prepare Heterogeneous and Homogeneous Catalysts”, NTS Inc., ISBN 978-4-86043-377-2 (in Japanese).

Chapter 4

Carbon Combustion Synthesis Ironmaking from Carbon-Infiltrated Goethite Ore

※ I defer the publication of this chapter due to submission to a scientific journal.

Chapter 5

General Conclusion

The ironmaking industry is facing three significant problems about resource (degraded high grade iron ore), energy (a lot of unutilized high-temperature waste heat), and environment (CO_2 emission). Goethite (FeOOH) ore, which has relative low iron contents because of combined water, has been utilized as an alternative raw material of high-grade iron ore. Goethite ore in the actual ironmaking process is heated at high temperature in the sintering process before it is put into blast furnace. However, the goethite ore becomes nanoporous after mild calcination at around 300℃. In this study, processes to solve the problems of the ironmaking industry using this nanoporous goethite-based ore were proposed and examined; (1) Ni-containing goethite ore utilization as a catalyst for the dry reforming of methane and (2) coke free fast ironmaking method using carbon infiltrated goethite ore.

Chapter 1 provided the general introduction of this thesis.

Chapter 2 described Ni-containing goethite (limonite) ore as a catalyst for the dry reforming of methane ($CH_4 + CO_2 \rightarrow 2H_2 + 2CO$). Ni-based catalysts are generally

utilized in this reaction, however, the production processes are very complex and the conventional catalysts are expensive to produce. In this study, cheap limonite ore catalyst was focused on and the catalytic performance of the limonite ore was observed. Goethite based ores which have different amounts of Ni were prepared. The ores were compared their catalytic performance by catalytic tests at several conditions. The ore containing larger amount of Ni showed higher catalytic performance, meaning the Ni in the ore effectively worked as a catalyst in the dry reforming reaction. The catalytic performance of the limonite ore was compared with Ni-supported goethite ore by wet impregnation method. They had almost same Ni amount, however, the limonite ore showed much higher catalytic performance. That was because the different sizes of Ni particle in the ores. TEM-EDS observation revealed that Ni in the limonite ore was homogeneously distributed and the supported Ni had larger size around 20 nm.

Chapter 3 described the effects of hydrogen reduction on the catalytic performance of the limonite ore in the dry reforming reaction. The main phase of the limonite ore after mild calcination is iron Fe_2O_3 and the Fe_2O_3 can be easily reduced in hydrogen or carbon monoxide atmosphere. This caused the different reduction degrees of the limonite ore during the catalytic tests. In this study, pre-reduction and hydrogen flowing during catalytic tests were tried to control the reduction degrees of the limonite ore and the effects of reduction were observed. When iron existed as oxides, Ni surface area drastically decreased because Ni segregation occurred during the catalytic tests. On the

other hand, when iron existed as metal, Ni surface area was very high because Ni and Fe formed bimetallic Fe-Ni and Ni distributed homogeneously in the alloy. Due to the higher Ni surface area, the limonite ore with high reduction degree showed higher catalytic performance.

Chapter 4 described proposal of a fast ironmaking method using carbon infiltrated goethite ore in an oxygen atmosphere, “combustion synthesis ironmaking”, and the probability of the combustion synthesis ironmaking theoretically and experimentally.

APPENDIX

Publications

1. ***Keisuke Abe***, Asami Kikuchi, Noriyuki Okinaka, Tomohiro Akiyama, "Single Thermite-type combustion synthesis of Fe_2VAl for thermoelectric applications from Fe, V_2O_5, and Al powders", Journal of Alloys and Compounds, 611 (2014), 319-323.

2. ***Keisuke Abe***, Genki Saito, Takahiro Nomura, Tomohiro Akiyama, "Limonitic Laterite Ore as a Catalyst for the Dry Reforming of Methane", Energy and Fuels **30** (2016), 8457-8462.

3. ***Keisuke Abe***, Ade Kurniawan, Takahiro Nomura, Tomohiro Akiyama, "Effects of Reduction on the Catalytic Performance of Limonite Ore for Dry Reforming Reaction", Journal of Energy Chemistry, in press.

Presentations (Domestic)

1. ***Keisuke Abe***, Asami, Kikuchi, Noriyuki Okinaka, Tomohiro Akiyama, "Single Thermite-type Combustion Synthesis of Fe_2VAl", The Mining and Materials Processing Institute of Japan, Hokkaido University, 3-5 September, 2013

2. ***Keisuke Abe***, Asami, Kikuchi, Noriyuki Okinaka, Tomohiro Akiyama, "Single Thermite-type Combustion Synthesis of Fe_2VAl for Thermoelectrics", 166th The Iron and Steel Institute of Japan, Kanazawa University, 17-19 September, 2013

3. ***Keisuke Abe***, Asami, Kikuchi, Noriyuki Okinaka, Tomohiro Akiyama, "Effects of ball-milling time on the Thermal Conductivity of Combustion Synthesized and Spark Plasma Sintered Fe_2VAl", Summer Session of The Japan Institute of Metals and Materials and The Iron and Steel Institute of Japan, Hokkaido University, 28 July, 2014

4. ***Keisuke Abe***, Asami, Kikuchi, Noriyuki Okinaka, Tomohiro Akiyama, "Synthesis of Heusler Alloy Fe_2VAl by Combustion Synthesis and Spark Plasma Sintering", 11th Annual Meeting of the Thermoelectrics Society of Japan, National Institute for Materials Science, Tsukuba, 29-30 September, 2014

5. ***Keisuke Abe***, Rochim Bakti Cahyono, Takahiro Nomura, Tomohiro Akiyama, "Chemical Vapor Infiltration (CVI) Ironmaking Process Using Pisolite Ore and Some Carbon Sources", 1st Ironmaking 54 Committee of Japan Society for the Promotion of Science, Hokkaido University, 2-3 July, 2015

6. ***Keisuke Abe***, Takahiro Nomura, Tomohiro Akiyama, "Catalytic properties of Ni-containing porous iron ore", 47th Autumn Meeting of The Society of Chemical Engineers Japan, Hokkaido University, 9-11 September, 2015

7. ***Keisuke Abe***, Genki Saito, Takahiro Nomura, Tomohiro Akiyama, "Catalytic performance of Ni-containing porous iron ore in the CO_2 reforming of methane", Winter Session of The Japan Institute of Metals and Materials and The Iron and Steel Institute of Japan, Hokkaido University, 17-18 December, 2015

8. ***Keisuke Abe***, Genki Saito, Takahiro Nomura, Tomohiro Akiyama, "Catalytic application of Ni-contained low grade iron ore", 171st The Iron and Steel Institute of Japan, Tokyo University of Science, 23-25 March, 2016

9. ***Keisuke Abe***, Ade Kurniawan, Takahiro Nomura, Tomohiro Akiyama, "Catalytic performance of laterite ore after hydrogen reduction", 172nd The Iron and Steel Institute of Japan, Osaka University, 21-23 September, 2016

10. ***Keisuke Abe***, Ade Kurniawan, Kouichi Ohashi, Takahiro Nomura, Tomohiro Akiyama, “Feasibility of Ironmaking by Carbon Combustion Synthesis”, 174th The Iron and Steel Institute of Japan, Hokkaido University, 7-9 September, 2017

Presentations (International)

1. ***Keisuke Abe***, Asami Kikuchi, Noriyuki Okinaka, Tomohiro Akiyama, "Thermite-Type Combustion Synthesis of Heusler-Alloy Fe_2VAl for Thermoelectric Materials", 3rd International Doctoral Student Symposium on Material Science (IDSS-3), Hokkaido University, 25-28 February, 2015

2. ***Keisuke Abe***, Genki Saito, Takahiro Nomura, Tomohiro Akiyama, "Catalytic application of Ni-containing low grade iron ore", The 14th Symposium between University of Science and Technology of Beijing & Hokkaido Univeristy, University of Science and Technology of Beijing, 6-9 March, 2016

3. ***Keisuke Abe***, Ade Kurniawan, Takahiro Nomura, Tomohiro Akiyama, "Hydrogen Generation via Some Catalytic Reactions over Limonite Ore", 1st International Conference on Energy and Materials Efficiency and CO_2 Reduction in the Steel Industry (EMECR2017), Kobe International Conference Center, 11-13 October, 2017

Awards

1. Tomohiro Akiyama, Asami Kikuchi, ***Keisuke Abe***, Noriyuki Okinaka, "Best Paper Prize of The 7th International Exergy, Energy and Environment Symposium", 30 April, 2015.

2. ***Keisuke Abe***, Rochim Bakti Cahyono, Takahiro Nomura, Tomohiro Akiyama, "Encouragement Prize of 1st Ironmaking 54 Committee of Japan Society for the Promotion of Science", 3 July, 2015.

3. ***Keisuke Abe***, Genki Saito, Takahiro Nomura, Tomohiro Akiyama, "Encouragement Prize of Winter Session of The Japan Institute of Metals and Materials and The Iron and Steel Institute of Japan", 18 December, 2015.

4. ***Keisuke Abe***, Genki Saito, Takahiro Nomura, Tomohiro Akiyama, "Effort Award of 171st The Iron and Steel Institute of Japan", 24 March, 2016.

5. ***Keisuke Abe***, Ade Kurniawan, Kouichi Ohashi, Takahiro Nomura, Tomohiro Akiyama, "Effort Award of 174th The Iron and Steel Institute of Japan", 8 September, 2017.